CHAPTER XI *PHASE TRANSFORMATIONS I: SOLIDIFICATION*

11.1 Introduction

A remarkable, though nonexclusive, property of metals is their ability to form alloys, i.e., solids formed by a mixture of atomic components. This mixture gives rise to phases that are mixtures of solids with physically and chemically homogeneous properties. The chemical composition of phases can be well defined (e.g., line compounds with clear stoichiometry, such as Ni3Al, CuAu, etc.). That is, intermediate or variable phases can be solid solutions in which supersaturation of the constituents can occur. Generally, intermediate phases have defined crystal structures (chemically ordered alloys) but can sometimes form amorphous solids or quasi-crystals. What distinguishes an intermediate phase from chemical compounds (i.e., molecules) is that it typically exists as large aggregates comprising many atoms, with some short-range chemical ordering. In contrast, a molecule can exist as a compound containing only two atoms. We must note that this description of an "alloy" can be extended to other materials, such as ceramics, composites, and polymers.

The concept of a phase is related to the stability of a thermodynamic system. This chapter defines the formalism necessary to understand how phases form under different conditions, using the classic thermodynamic parameters and the composition or concentration of their constituents. We then specifically explain how phases form (Solidification and phase transformations in the solid state), and how this governs their morphology and microstructure.

11.2 Thermodynamics background

We consider a binary alloy formed of N_A atoms of type A and N_B atoms of type B. $X_A = \frac{N_A}{N_A + N_B}$ is the concentration of A and $X_B = \frac{N_B}{N_A + N_B} = 1 - X_A$ is the concentration of B.

Since we consider the system's evolution at given temperature and pressure conditions, we use the minimum Gibbs free energy as a criterion. The variation in this energy, ΔG_m, is given by the heat emitted or absorbed during the reaction, ΔH_m, and by the change in entropy of the mixture, ΔS_m. Thus:

$$\Delta G_m = \Delta H_m - T\Delta S_m \tag{11.1}$$

11.2.1 Calculation of the mixing entropy (ideal solid solution)

Suppose now that $\Delta H_m = 0$, which means that a net-zero energy balance is required to bind the atoms to one another, i.e., an ideal solution. The mixing entropy is given by the number of possibilities of distributing N_A or N_B on N lattice sites.

$$T\Delta S_m = kT\ln\left(\frac{(N_A+N_B)!}{N_A!N_B!}\right) \rightarrow \text{(using the Stirling formula } \ln N! \approx N\ln N - N\text{)}$$

$$= kT[(N_A+N_B)\ln(N_A+N_B) - N_A lnN_A - N_B lnN_B]$$

Considering a mole of solution $N_A = X_A n_a$, where n_a is Avogadro s constant:

$$T\Delta S_m = kT[n_a(X_A+X_B)[\ln n_a + \ln(X_A+X_B)] - n_a(X_A(\ln n_a + \ln X_A) + X_B(\ln n_a + \ln X_B))]$$

As $X_A + X_B = 1$, we can simplify this in:

$$T\Delta S_m = kT[-n_a(X_A lnX_A + X_B lnX_B)] = -RT(X_A lnX_A + X_B lnX_B) \quad (11.2)$$

The total free energy of the mixture is given by:

$$G = G_A X_A + G_B X_B + RT(X_A lnX_A + X_B lnX_B) \quad (11.3)$$

But we know from the definition that $G = \mu N$ (from eqn. 3.37), which in terms of molar energy gives:

$$G = \mu_A X_A + \mu_B X_B \quad (11.4)$$

By setting (11.3) and (11.4) equal, we get:

$$\begin{aligned} \mu_A &= G_A + RTlnX_A \\ \mu_B &= G_B + RT\ln X_B \end{aligned} \quad (11.5)$$

where we can recognize the expressions describing the thermodynamic equilibrium of a chemical reaction. Equation (11.4) is equivalent to describing $G(X_B)$ as being enveloped by its tangents.

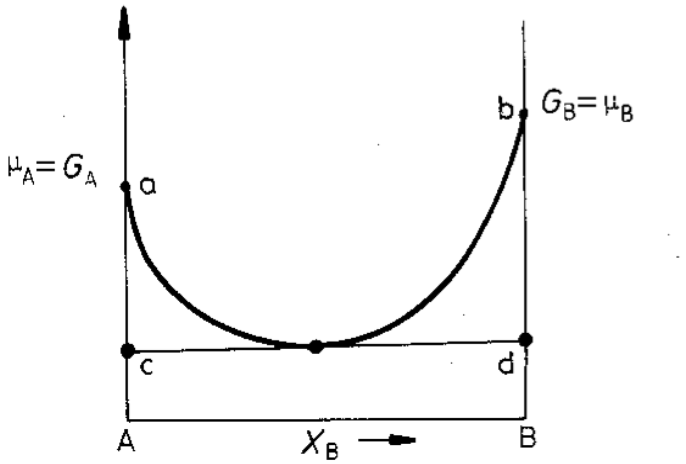

Figure 11-1: *Relation between free energy and chemical potential.*

11.2.2 Formation heat or mixing enthalpy ΔH_m calculation (real solution)

The bond energy between neighboring atoms must be considered in a solid solution.

Here, we consider a binary alloy A+B, in which we randomly place A and B atoms in the alloy. This type of alloy implies that the two kinds of atoms have somewhat similar properties.

Let: V_{AA} = A-A interaction potential
V_{AB} = A-B interaction potential
V_{BB} = B-B interaction potential

In all cases:

$$\Delta H_m \sim \Delta E_m = N_{AA}V_{AA} + N_{BB}V_{BB} + N_{AB}V_{AB} \tag{11.6}$$

where N_{AA} is the number of A-A pairs,

$$N_{AA} = NX_A \cdot zX_A \cdot \frac{1}{2} \tag{11.7}$$

and z is the coordination number.

$$N_{AA} = \frac{1}{2}NzX_A^2 \tag{11.8}$$

Thus:

$$N_{BB} = \frac{1}{2}NzX_B^2$$

Similarly:

and

$$N_{AB} = NzX_AX_B \tag{11.9}$$

If we express the concentration of the alloy in terms of the element A, we can write:

$$X_A = X \text{ and } X_B = 1 - X_A$$

Substituting in (11.8), we get:

$$N_{AA} = \frac{1}{2}NzX^2 \tag{11.10}$$

$$N_{BB} = \frac{1}{2}Nz(1-X)^2 \tag{11.11}$$

$$N_{AB} = NzX(1-X) \tag{11.12}$$

Then:

$$\Delta H_m \cong \Delta E_m = \frac{1}{2}NzX^2V_{AA} + \frac{1}{2}Nz(1-X)^2V_{BB} + NzX(1-X)V_{AB} =$$

$$= \frac{1}{2}Nz[XV_{AA} - X(1-X)V_{AA} + (1-X)V_{BB} - X(1-X)V_{BB} + 2X(1-X)V_{AB}] =$$

$$= \frac{1}{2}Nz[XV_{AA} + (1-X)V_{BB} + 2X(1-X)\left(V_{AB} - \frac{V_{AA}+V_{BB}}{2}\right)$$

Now, letting , $V = V_{AB} - \frac{V_{AA}+V_{BB}}{2}$ which is the additional energy term due to the mixing (see Figure 11-3), ΔH_m becomes:

$$\Delta H_m = \frac{1}{2}Nz[XV_{AA} + (1-X)V_{BB} + 2X(1-X)V] \tag{11.13}$$

We can distinguish three cases:

1) $V = 0$, that is to say, $V_{AA} \sim V_{AB} \sim V_{BB}$

2) Close neighbor atoms are of type A or B indifferently: the solid solution is disordered. $V > 0$ or $V_{AB} > \frac{V_{AA} + V_{BB}}{2}$, that is V_{AA} and $V_{BB} < V_{AB}$

The atoms of the same type tend to agglomerate. Thus, phases (α and β) segregate in regions with different chemical compositions. A heterogeneous mix is then obtained (Figure 11-2).

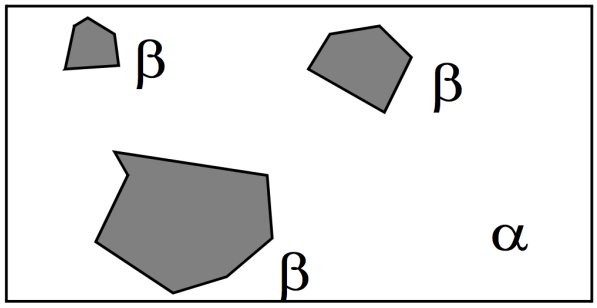

Figure 11-2: *Heterogeneous mixture*

3) $V < 0$ or $V_{AB} < \frac{V_{AA} + V_{BB}}{2}$ that is $V_{AB} < V_{AA}$ and V_{BB}

In this third case, the atoms rearrange so that their neighboring atoms are other species because it is the most energetically favorable. We then obtain an ordered solid solution, possibly forming very stable chemical compounds (stoichiometric line compounds).

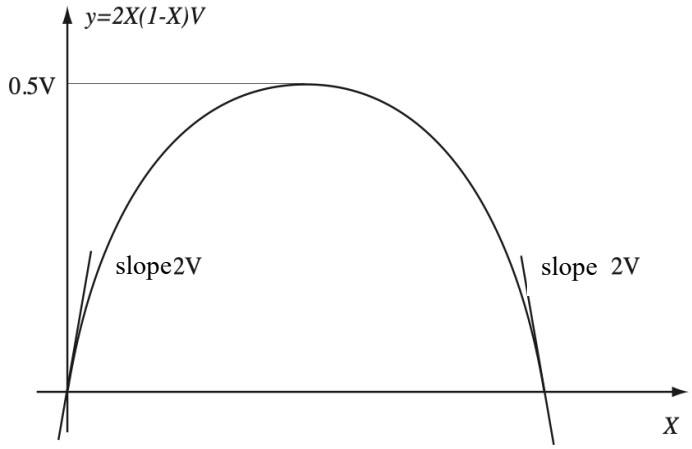

Figure 11-3: *Graph of the function 2X (1-X) V with V>0.*

In terms of molar concentrations X_A and X_B, the interaction term above can be written:

$$NzX(1-X)V = \Omega X_A X_B = \Omega(X_A^2 X_B + X_A X_B^2) = \Omega(X_A(1-X_A)^2 + X_B(1-X_B)^2) \qquad (11.14)$$

and equation (11.13) can be written as:

$$\Delta H_m = G_A X_A + G_B X_B + \Omega X_A X_B \qquad (11.15)$$

Thus:

$$\Delta G_m = \Delta H_m - T\Delta S_m = G_A X_A + G_B X_B + \Omega X_A X_B + RT(X_A lnX_A + X_B lnX_B) \qquad (11.16)$$

Summing the terms of (11.16), excluding the self-energy terms $G_A X_A + G_B X_B$, is represented in Figure 11-4. The mixing enthalpy term is the one illustrated in Figure 11-3. According to the sign of V, ΔH_m can have positive or negative curvature. On the other hand, the mixing entropy term, given in equation (11.2), is always positive.

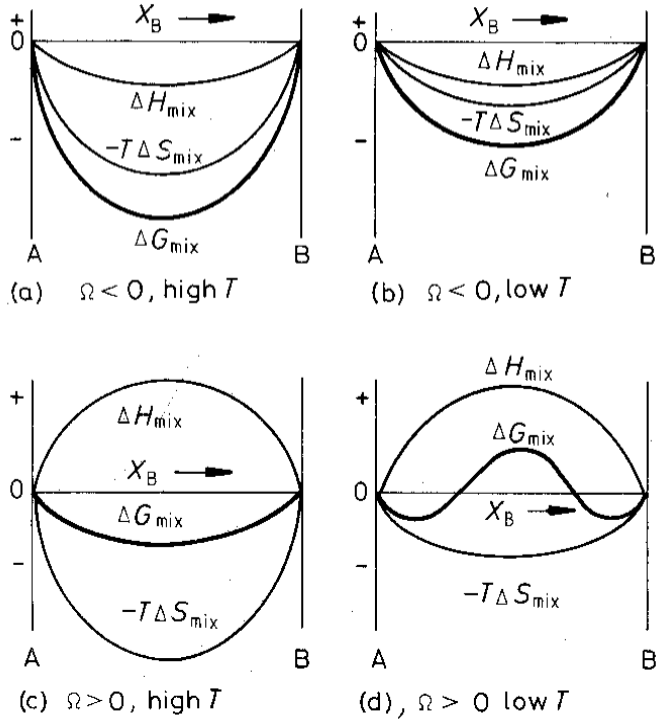

Figure 11-4: *Free energy of the mixture ΔG_m as a function of the mixing enthalpy variations and the mixing entropy*

11.2.3 Chemical potential and activity

Considering the expression of the free energy in terms of chemical potentials of equation (11-4) and the expression for the formation heat (enthalpy) of the mixture, we can express the chemical potentials of a regular solution as:

$$\begin{aligned} \mu_A &= G_A + \Omega(1 - X_A)^2 + RT \ln X_A \\ \mu_B &= G_B + \Omega(1 - X_B)^2 + RTlnX_B \end{aligned} \qquad (11.17)$$

It is possible to reduce these expressions into the simpler form obtained for ideal solutions by introducing the activity, a_A, of a substance A in the solution and defining:

$$\mu_A = G_A + RT \ln a_A \qquad (11.18)$$

$$\mu_B = G_B + RT \ln a_B \qquad (11.19)$$

Thus:

$$\ln\frac{a_A}{X_A}=\frac{\Omega}{RT}(1-X_A)^2 \quad \text{and} \quad \ln\frac{a_B}{X_B}=\frac{\Omega}{RT}(1-X_B)^2 \tag{11.20}$$

The ratio

$$\frac{a_A}{X_A} = \gamma_A \tag{11.21}$$

is usually called the activity coefficient. If $\gamma_A < 1$ an exothermic reaction occurs ($\mu_A < G_A$), the mixture tends to form stable compounds. If an endothermic reaction occurs, heat must be supplied to drive the mixing. If $\gamma_A = 1$ we have an ideal solution (Raoult law). For small concentration ranges, we can consider $\gamma_A \approx const$ (Henry s law)

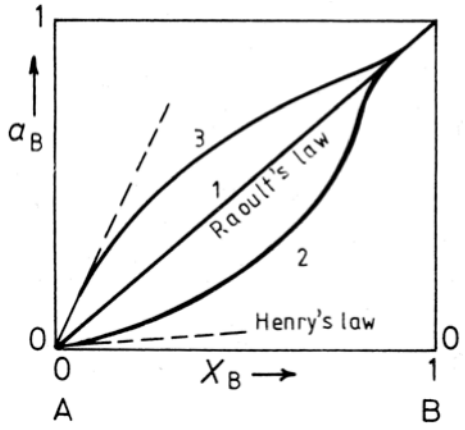

Figure 11-5: *Activity as a function of concentration*

11.3 Binary phase diagrams

11.3.1 Chemical potential

Components A and B often do not have the same crystal structure in pure solids. As such, the free energy of the solution of B atoms in A must be derived. For example, B atoms adopt an unstable configuration within the crystal structure of A. This increases the free energy proportionally to the concentration of B. We perform the same analysis for atoms of A in B (Figure 11-6). We must consider two phases, α and β, with a chemical potential given by equation (11.5) or, more generally, by equations (11.18) and (11.19). For example, in the case of an ideal solution:

$$\mu_A^\alpha = G_A^\alpha + RT \ln X_A^\alpha \tag{11.22}$$

$$\mu_A^\beta = G_A^\beta + RT \ln X_A^\beta \tag{11.23}$$

11.3.2 Free energy of a mixture of phases

Consider a binary alloy A+B with a species B concentration: $X_B = X_0$.

A simplified notation is used in the following paragraph, and index B is dropped because we are only concerned with this species. We also note that in this paragraph, we use the notation X" to indicate the concentration (volume, molar, or %) of a constituent and f" to indicate the proportion of a phase.

Let f^α the proportion of alloy with concentration X^α

f^β the proportion of alloy with concentration X^β

with $f^\alpha + f^\beta = 1$.

Then, the concentration of the alloy with concentration X is expressed as:

$$X = f^\alpha X^\alpha + f^\beta X^\beta = f^\alpha X^\alpha + (1 - f^\alpha) X^\beta$$

We deduce that:

$$f^\alpha = \frac{X^\beta - X}{X^\beta - X^\alpha} \text{ and } f^\beta = 1 - f^\alpha = \frac{X - X^\alpha}{X^\beta - X^\alpha} \tag{11.24}$$

The free energy of the alloy with concentration X is expressed as a linear combination of the free energies of the phases α and β:

$$G = f^\alpha G^\alpha + f^\beta G^\beta = \frac{X^\beta - X}{X^\beta - X^\alpha} G^\alpha + \frac{X - X^\alpha}{X^\beta - X^\alpha} G^\beta$$

$$G = G^\alpha + (G^\beta - G^\alpha) \frac{X - X^\alpha}{X^\beta - X^\alpha} \tag{11.25}$$

G_{min} is given by the common tangent" to the curves α and β (Figure 11-6):

$$G_{min}^{(c)} = G_{c_1}^\alpha + (G_{c_2}^\beta - G_{c_1}^\alpha) \frac{X - X_1}{X_2 - X_1}$$

If X varies between X_1 and X_2, the concentrations of the phase components do not:

in α, we have: X_1^A and $X_1^B = 1 - X_1^A$

in β, we have: X_2^A and $X_2^B = 1 - X_2^A$

However, f^α and f^β do vary:

$$f^\alpha = \frac{X_2 - X}{X_2 - X_1} \text{ and } f^\beta = \frac{X - X_1}{X_2 - X_1}$$

Remark

As μ_A^α and μ_A^β or μ_B^α and μ_B^β define the tangent lines to the energy minimum (Figure 11-1), we can identify the following chemical potentials,

$$\mu_A^\alpha = \mu_A^\beta \text{ and } \mu_B^\alpha = \mu_B^\beta \tag{11.26}$$

11.3.3 Phase Diagrams Construction

The energy minimization described in the prior section is at the heart of constructing phase diagrams. Figures 11-7 and 11-9 give us two examples. The common tangent, which defines the energy minimum (11-6), allows us to identify the most stable phases and their proportions. We note that as the temperature decreases, the liquid phase becomes less stable and transforms into solid phases.

There is a common tangent between the three phases at a specific temperature; this temperature is called the eutectic temperature. It is the lowest melting point of the alloy.

Let us compare two typical cases in Figures 11-7 and 11-9. In Figure 11-7, the phases α and β exhibit two crystal structures. They illustrate a classic eutectic diagram with the decomposition into two solid-state phases.

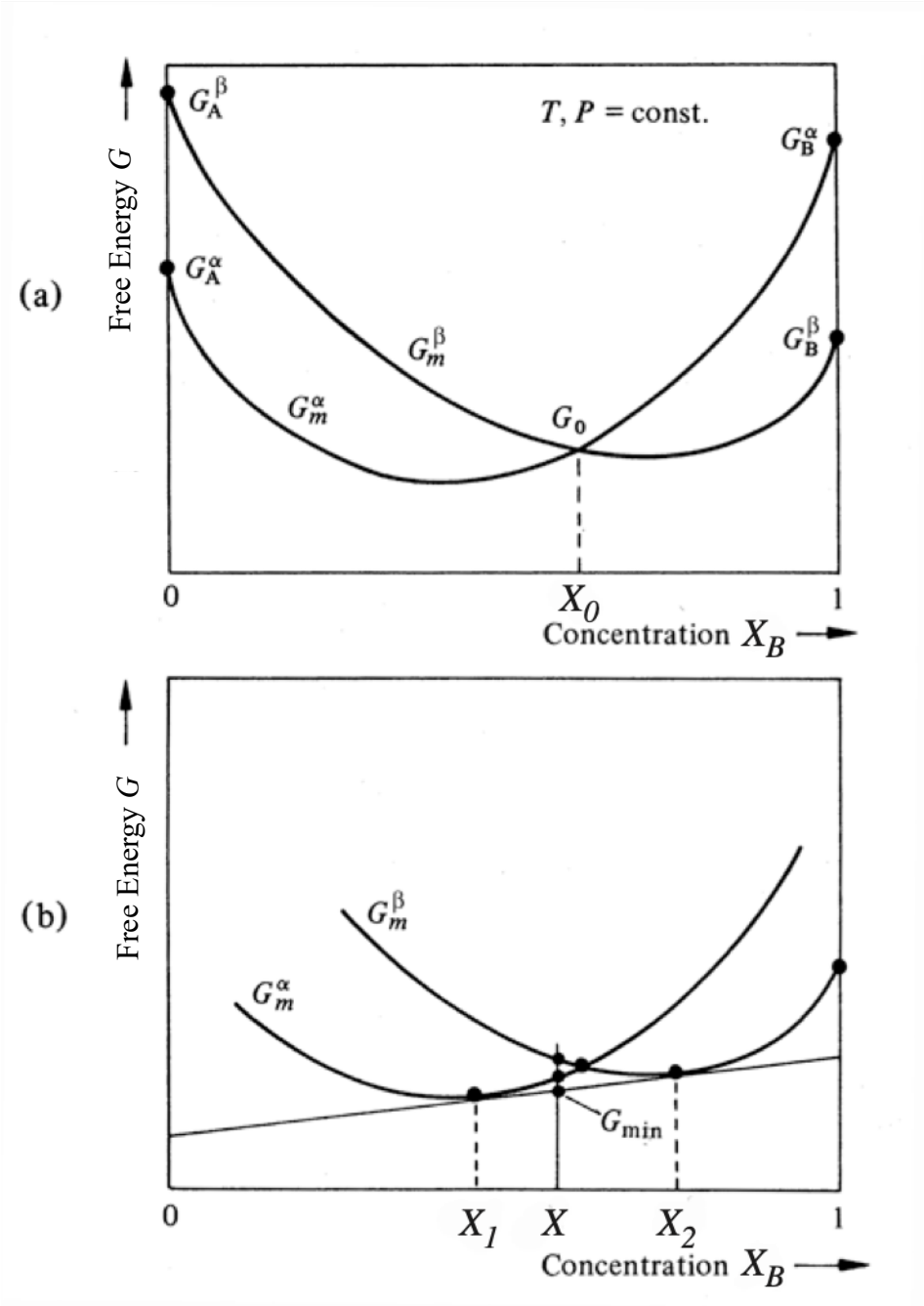

Figure 11-6: *Minimum energy diagram of a mixture of phases*

Figure 11-9 shows the phase diagram of an alloy composed of two phases with the same crystal structure but with solid-state mixing issues (Figure 11-8). We form a eutectic phase, but the region with negative free-energy curvature undergoes spinodal decomposition into two phases. The limits between the phases α_1 and α_2 and the mixture of phases are located on the common tangent (Figure 11-8): the solubility limit.

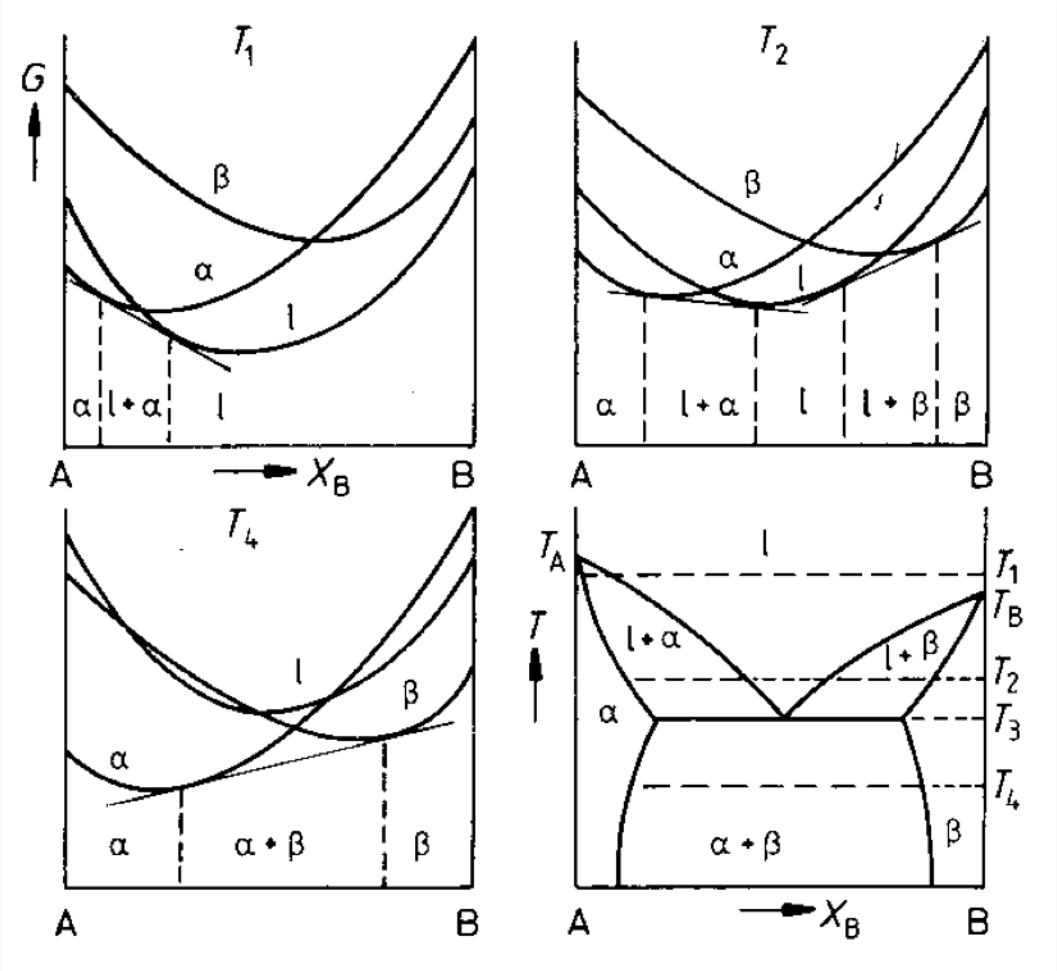

Figure 11-7: *Eutectic phase diagram, α, and β phases have different crystal structures*

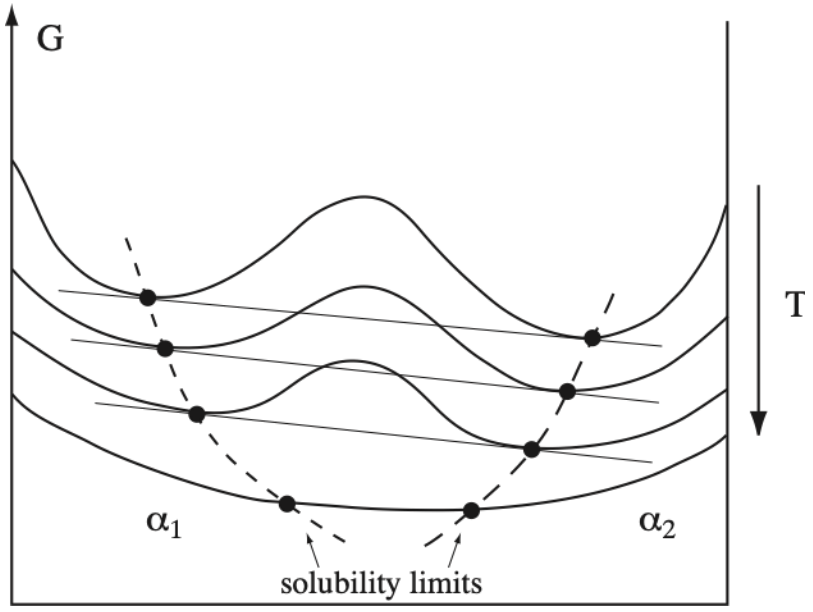

Figure 11-8: *Energy diagram and solubility limit*

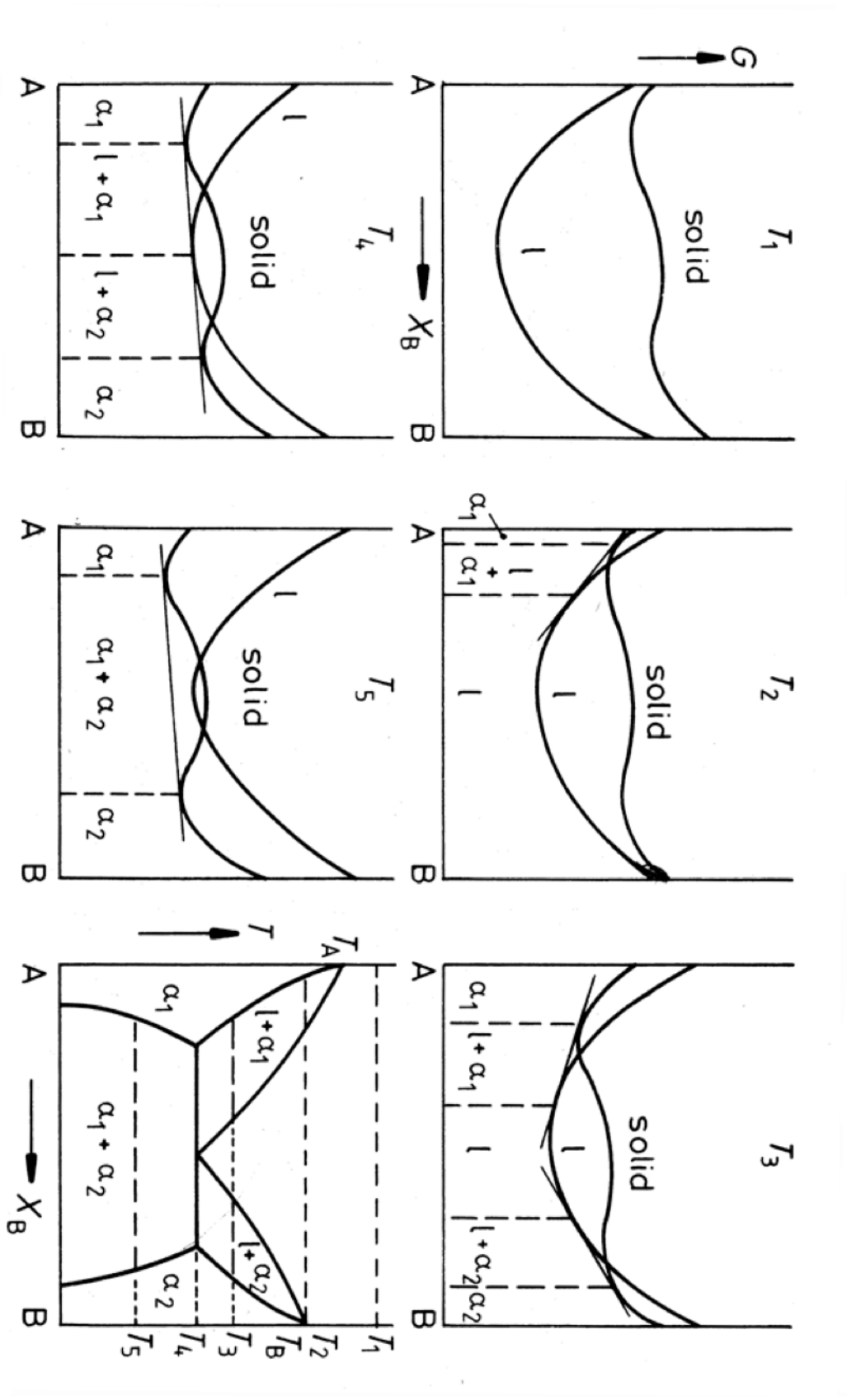

Figure 11-9: *Eutectic phase diagram, α_1 and α_2 or phases with the same crystal structure with a miscibility gap*

Spinodal decomposition

Consider an alloy quenched in the solid state in the decomposition zone $\alpha_1 + \alpha_2$. We note that two cases are possible if we look closely at the energy diagram (Figure 11-10). First, if the composition X_0 of the alloy is inside the zone defined by the inflection points of *G* such that $\left(\frac{\partial^2 G}{dx^2} = 0\right)$, any fluctuation decreases the initial energy G_0. Then, the alloy becomes unstable and immediately decomposes into two phases, without any potential barriers. The set of points defined by the inflection points as a function of temperature is called a spinodal curve. Suppose the composition of the alloy is between the solubility limit and the spinodal curve (/in Figure 11-10). In that case, any decomposition implies a potential barrier, and the precipitation of α_2 in α_1 is impossible without the nucleation of precipitates, as discussed in Chapter XII.

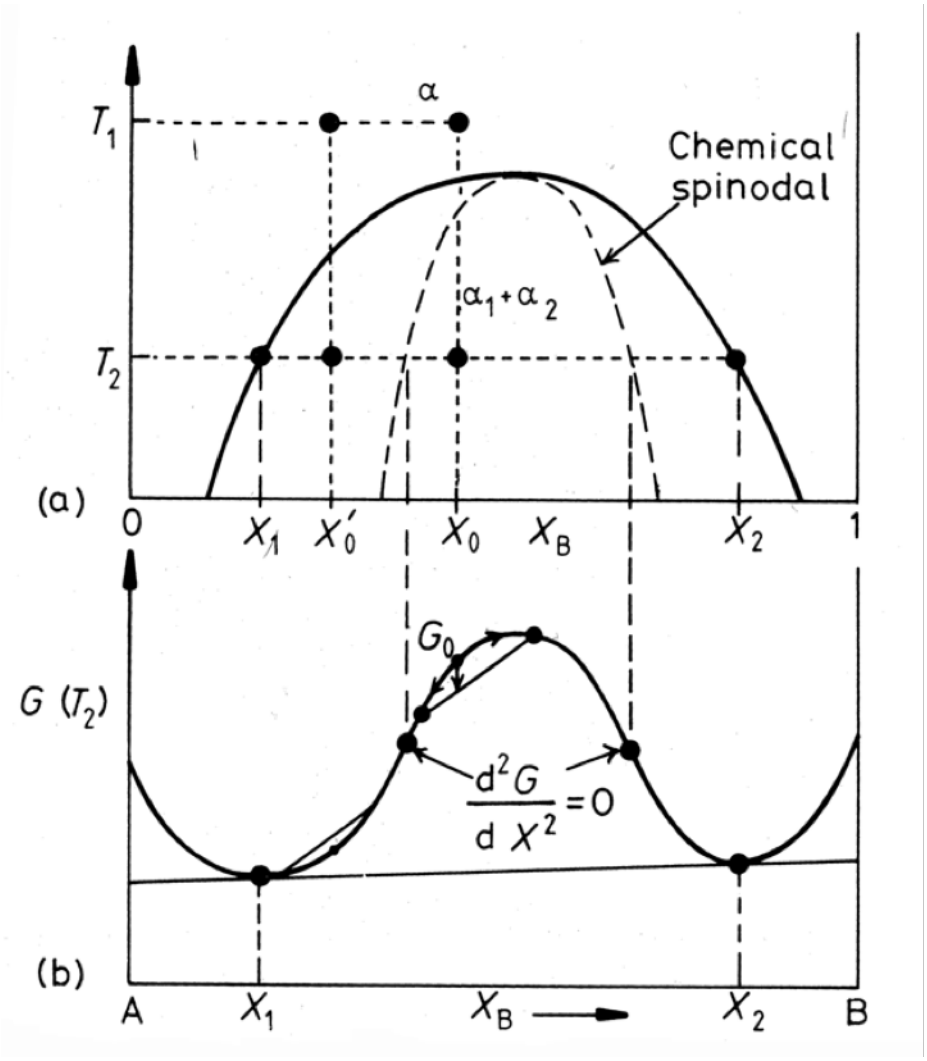

Figure 11-10: *Spinodal decomposition*

11.4 Solidification

From the metallurgical point of view, solidification is undoubtedly the most important transformation. The production of metals and metallic alloys almost always involves a solidification process, e.g., producing rare ingot alloys and cast parts. Therefore, it is fundamental for engineers and material physicists to develop and improve solidification processes to produce homogeneous materials with desired, uniform compositions, free of macroscopic defects, and with homogeneous physical, chemical, and mechanical properties. Variations in the chemical composition within the solidified ingots lead to detrimental mechanical properties and lower corrosion resistance or fatigue resistance. Therefore, it is vital to understand the fundamental physical and chemical mechanisms of solidification to design desired material properties and ensure quality control. Thus, we must have detailed knowledge of solidification processes, nucleation and growth, interface morphology, and segregation.

In a liquid, atoms (or molecules) vibrate at a frequency ν with an average energy of 3/2 kT. In a solid, atoms also have an average vibrational energy of 3/2 kT. The difference is that the neighboring atoms change more often in a liquid than in a solid (high diffusivity). In a liquid, atoms can be displaced over long distances.

Solidification is a first-order transformation, meaning there is a discontinuity in the first derivatives of energy: *V* and *S.* Table XI-1 shows that, in most cases, the volume variation during solidification is negative. That is, the liquid density is lower than that of the solid. The arrangement of the atoms in a liquid is more disordered than in a solid (compact or pseudo-compact structures). Heat must be supplied to melt a solid into a liquid: **the latent heat of melting *L***, which takes entropy variation (positive) into account.

Table XI-1: *Volume change of different elements during solidification* $\Delta V = V_{Sol} - V_{Liq}$

Element	ΔV (in %)
Al	-6
Mg	-5.1
Cd	-4.7
Zn	-4.2
Cu	-4.1
Ag	-3.8
Hg	-3.7
Pb	-3.5
Sn	-2.8

Na	-2.5
K	-2.5
Fe	-2.2
Li	-1.65
Sb	+0.95
Ga	+3.2
Bi	+3.3

a) Latent heat

The free energy of a liquid per unit volume is: $G_L = H_L - TS_L$
The free energy of a solid per unit volume is: $G_S = H_S - TS_S$

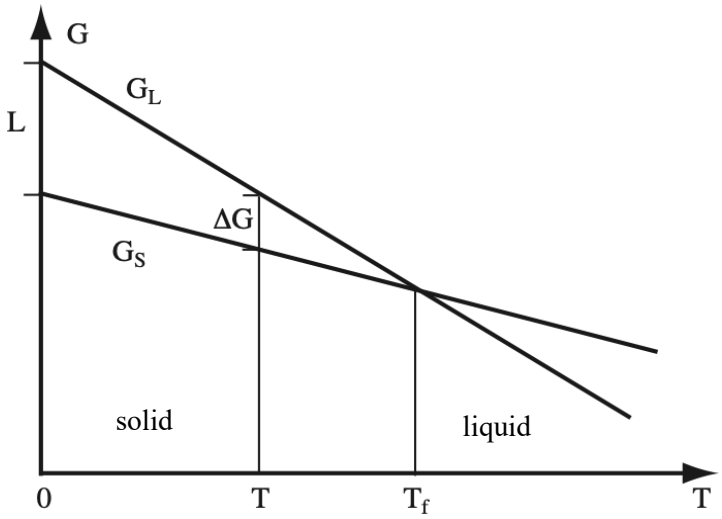

Figure 11-11: *Diagram showing the equilibrium energy of solid phases and liquid phases schematically*

At melting temperature (or solidification temperature), we have $G_L = G_S$, which in turn implies:

$$H_L - T_F S_L = H_S - T_S S_S \tag{11.27}$$

$$\Delta H_F = H_L - H_S = T_F(S_L - S_S) = T_F \Delta S_F \tag{11.28}$$

$$\Delta H_F = H_L - H_S = L \tag{11.29}$$

L is the latent heat of melting. According to equation 11.29, this quantity is positive for the transition to the liquid phase. However, this energy is the heat liberated by the body during solidification, which is regarded as negative.

$$\Delta S_F = \frac{L}{T_F} \tag{11.30}$$

As the difference in order between a solid and a liquid is much bigger than between two solids, ΔS_F associated with solidification is relatively independent of the crystal structure.

Table XI-2: *Entropy change during the solidification of different metals*

Metal	Structure	Latent heat cal/mol	Melting point (˚K)	ΔS_F
Aluminum	FCC	2500	993	2.6
Copper	FCC	2700	1356	2
Lead	FCC	1300	600	2.2
Sodium	CC	635	370	1.7
Zinc	HCP	1560	693	2.3

b) Relation between volume and latent heat: Clausius-Clapeyron equation

If two phases α and β have different densities, their energies vary differently with temperature. Maintaining equilibrium during temperature changes involves adjusting pressure. The free energy once more dictates the equilibrium:

$$\begin{aligned} dG^\alpha &= V^\alpha dP - S^\alpha dT \\ dG^\beta &= V^\beta dP - S^\beta dT \end{aligned} \tag{11.31}$$

Since at equilibrium, $G^\alpha = G^\beta$, then $dG^\alpha = dG^\beta$ and thus:

$$\left(\frac{dP}{dT}\right)_{eq} = \frac{S^\beta - S^\alpha}{V^\beta - V^\alpha} = \frac{\Delta S}{\Delta V} \tag{11.32}$$

As seen before in (11.28), for solidification $\Delta G = \Delta H - T\Delta S = 0$. Therefore:

$$\left(\frac{dP}{dT}\right)_{eq} = \frac{\Delta H}{T_{eq}\Delta V} \tag{11.33}$$

This is the Clausius-Clapeyron relation. It gives the relation between pressure and temperature at equilibrium as a function of the latent heat ΔH and the volume variation (molar) between phases.

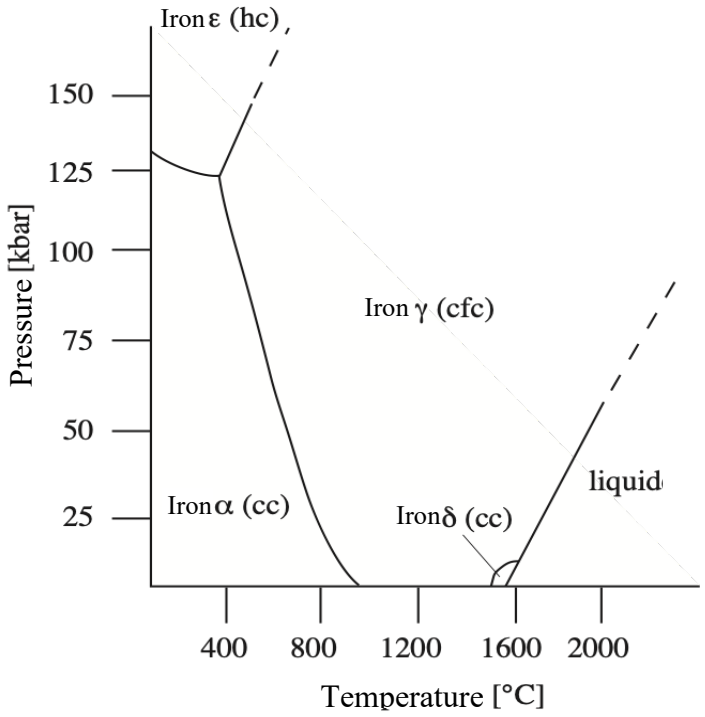

Figure 11-12: *Equilibrium diagram of iron*

If, as in the solidification of most materials (water being an exception), $\Delta H<0$ and $\Delta V<0$, we have $\left(\frac{dP}{dT}\right)_{eq}>0$.

Figure 11-12 shows that the equilibrium solid-liquid curve has a positive slope since the transformation from α iron and γ iron is endothermic. In contrast, if the volume of the γ phase is smaller than that of the α phase (FCC is more compact than CC structure), then the slope $\left(\frac{dP}{dT}\right)_{eq}$ is negative.

11.4.1 Nucleation

According to equilibrium thermodynamics, a liquid is not in equilibrium below its fusion point T_f. In reality, we can observe a metal in the liquid state under specific conditions, well below Tf (for example, we can achieve 250˚C of supercooling in Nickel).

Solidification is a process that occurs through nucleation and growth. In general, a *nucleus* can be defined as a group of atoms in the liquid phase with the same symmetry as the solid. Creating a nucleus requires the creation of a liquid-solid" interface, which implies positive free energy. This interface formation energy is due to supercooling.

At a temperature $T < T_F$, the excess of free energy ΔG is:

$$\Delta G = G_L - G_S = \Delta H_F - T(S_L - S_S) = L - T\Delta S_F \tag{11.34}$$

Taking into account (11.30):

$$\Delta G = L - T\frac{L}{T_F} = \frac{L}{T_F}\Delta T = \Delta S_F \Delta T \tag{11.35}$$

where $\Delta T = T_F - T$ is called supercooling.

The minimization of the formation energy of the liquid-solid interface leads to two kinds of nucleation:

- The general nucleation is the case where nuclei form randomly throughout the liquid
- Localized nucleation occurs when nuclei form on preferential sites.

a) Homogeneous nucleation

The formation of a nucleus of a solid requires a variation in free energy, which is made up of two terms, one related to the volume and the other to the surface:

$$\Delta G_g = \Delta g_v V + \Delta g_s s \tag{11.36}$$

The first term on the right of (11.36) is negative, whereas the second is positive.
If we suppose that the nucleus is spherical with a radius *r*:

$$\Delta G_g = (g_S - g_L)\frac{4}{3}\pi r^3 + 4\pi r^2\gamma = -\frac{4}{3}\pi r^3 \frac{L}{T_F}\Delta T + 4\pi r^2\gamma \tag{11.37}$$

with γ = specific free energy of the interface.

The radius giving the stability limit of the nucleus *r** is given by:

$$\frac{\partial \Delta G_g}{\partial r} = 0$$

and we get:

$$r^* = \frac{2\gamma T_F}{L\Delta T} \tag{11.38}$$

For the nucleation radius. The binding energy representing the potential barrier is:

$$\Delta G^* = \frac{16}{3}\pi\gamma^3 \frac{T_F^3}{L^2\Delta T^2} \tag{11.39}$$

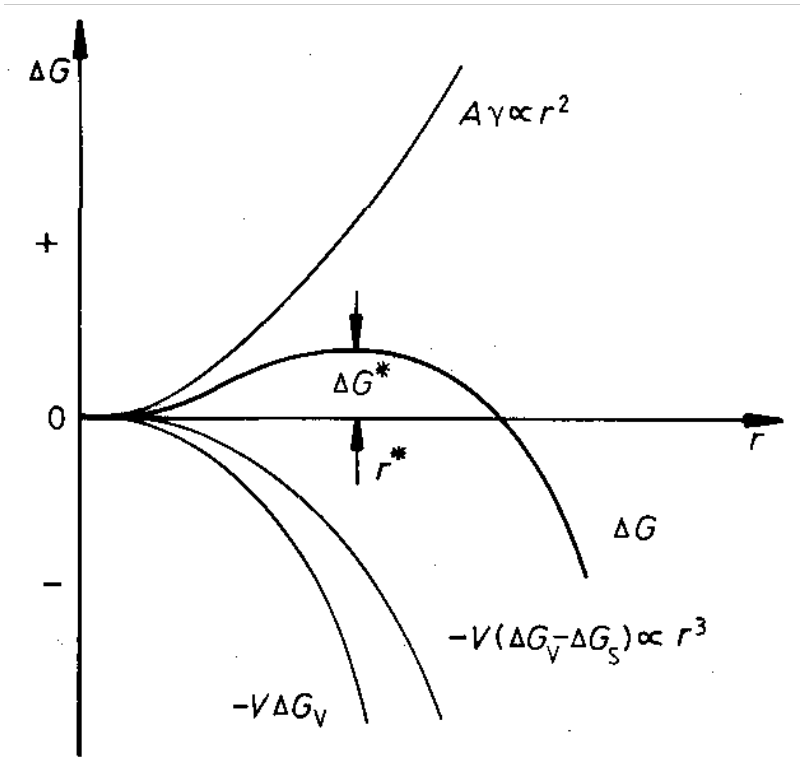

Figure 11-13: *Critical radius of nucleation*

At the temperature T_F, $\Delta T = 0$ and $\Delta G^* = \infty$, $r^* = \infty$.

Solidifying a pure liquid at the equilibrium temperature T_F is impossible. This agrees with experiments. We always need supercooling for a transformation to occur. If a nucleus were formed every second for solidification to begin (a reasonable estimate within an order of magnitude), a supercooling of 200 K would be required. In practice, extensive samples do not exhibit supercooling above 5 K, demonstrating the effectiveness of external particles as catalysts of the nucleation process. Localized nucleation (on an external particle or at the mold edges) requires a lower activation energy than general nucleation.

b) Localized nucleation

In most cases, solidification takes place in molds or solid crucibles. Nucleation then begins at the mold edges, where discontinuities such as cracks, porosities, and oxide films provide potential initiation sites. Inclusions or groups of impurities within the liquid metal can also serve as centers of early crystal growth.

Consider the formation of a solid nucleus on the plane surface of an external particle. The chemical forces determine the growth of this nucleus at the interfaces, which is represented by the surface tensions:

γ_{IL} = interface energy liquid-impurity
γ_{IS} = interface energy solid-impurity
γ_{SL} = interface energy solid-liquid

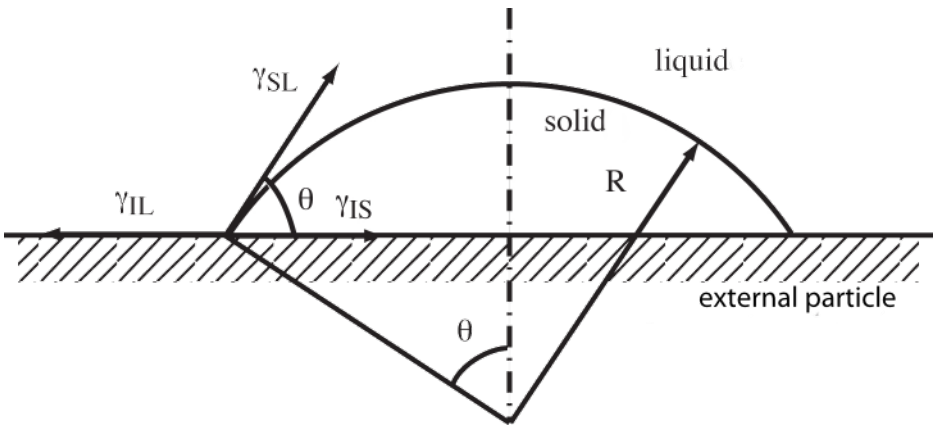

Figure 11-14: *Wetting phenomenon*

The equilibrium of surface tensions gives (Young s law):

$$\gamma_{IL} = \gamma_{IS} + \gamma_{SL} cos\theta \tag{11.40}$$

If $\gamma_{IS} > \gamma_{IL}$ the nucleus tends to be spherical
If $\gamma_{IS} < \gamma_{IL}$ the nucleus tends to spread on the surface

We can determine the free energy of formation and the radius of curvature of the critical nucleus (exercises):

$$R_c^{loc} = -\frac{2\gamma_{SL}}{\Delta g_V} \tag{11.41}$$

$$\Delta G_c^{loc} = \frac{4}{3}\pi \frac{\gamma_{SL}^3}{\Delta g_V^2}(2 - 3\cos\theta + \cos^3\theta) \tag{11.42}$$

We note that R_c^{loc} (loc" for localized) is independent of the angle θ. The critical radius is identical to that of the general nucleation. However, in the case of nucleation on a substrate, the number of atoms constituting the nucleus with curvature radius R_c^{loc} is much smaller. Therefore, ΔG_c^{loc} is proportional to the volume of the nucleus since $\gamma_{SL} \sim R_c^{loc}$ (11.41).

For θ = π, we have $\Delta G_c^{loc} = \Delta G_c^{gen}$: the solid does not wet the substratum, and the nucleus has only a point of contact with the surface.

For θ = 0, $\Delta G_c^{loc} = 0$: the solid wets perfectly the substratum (we have a thin film on the surface of the substratum). There is no barrier to nucleation. The required supercooling becomes zero.

Therefore, heterogeneity decreases, and consequently, supercooling is necessary for solidification. Moreover, the substratum's geometry or shape plays a non-negligible role. For instance, cracks on the surface decrease (ΔG_c), since the interface solid-liquid is decreased for an equal nucleation volume (Figure 11-15).

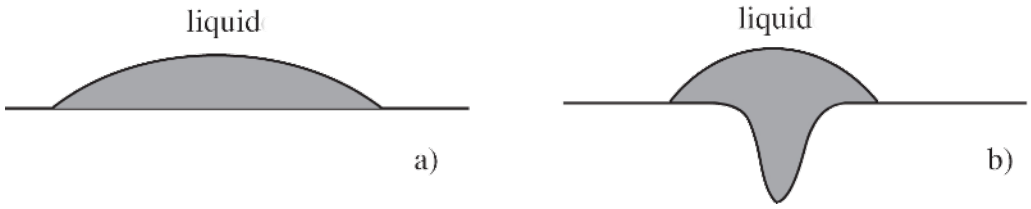

Figure 11-15: *Localized nucleation: a) on a smooth surface, b) in a crack*

11.4.2 Statistics of Nucleation

According to Boltzmann's statistics, we can write: $N^* = N_\alpha e^{-\frac{\Delta G^*}{kT}}$ (11.43)

with N^* = number of critical nuclei made up by *n* [atoms/cm^3]

N_α = number of possible sites for the creation of a nucleus/cm^3

ΔG^* = formation energy of a critical nucleus (11.39)

To grow a nucleus, we assume that a nucleus has a critical size of *n* atoms and that this nucleus captures one atom.

Then, the rate of nucleation I (the number of nuclei per unit volume and per unit time) can be written:

$$I = N^* \cdot n_s \cdot \nu_C$$

with N^* = number of embryos of n atoms/cm^3
n_S = number of atoms at the interface
ν_C = capture frequency

$$\nu_C = \nu_D z e^{-\frac{\Delta G^S}{kT}} \tag{11.44}$$

with ν_D = Debye frequency
ΔG^S = activation energy of an atomic jump (migration energy)
z = coordination number

Then:

$$I = I_0 e^{-\frac{\Delta G^* + \Delta G^S}{kT}} \tag{11.45}$$

Now, equation (11.39) implies that:

$$\Delta G^* = \frac{16}{3}\pi\gamma^3 \frac{T_F^2}{L^2} \frac{1}{(T - T_F)^2}$$

for $T \to T_F$ $\quad \Delta G^* \to \infty$ and $I \to 0$
for $T \to 0$ $\quad I \to 0$

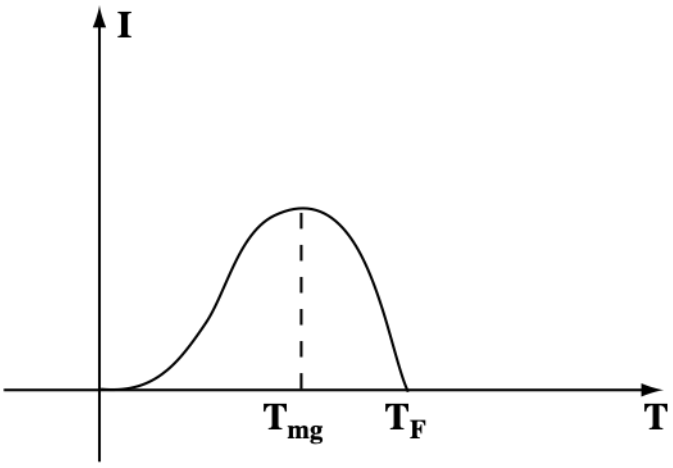

Figure 11-16: *The nucleation rate has a maximum for T_{mg}*

The nucleation rate has a maximum for I_{max} for $T = T_{mg}$ and is defined by $dI/dT = 0$. The shape of the curve depends on the ratio between ΔG_n^* and ΔG^S and on their variation as a function of temperature.

11.4.3 TTT curves (Time-Temperature-Transformation diagrams)

Let α be a parameter, α = # of nuclei/cm^3. To reach a specific value of α, we must wait for a time t such that $\alpha = I\,t$. We can write (11.45):

$$\log t = \log\frac{\alpha}{I_0} + \frac{\Delta G^*}{k}\frac{1}{T} + \frac{\Delta G^S}{k}\frac{1}{T} \tag{11.46}$$

For $T \to T_F$: $I \to 0$ and $\frac{\alpha}{I} \to \infty$, thus $\log t \to \infty$

For $T \to 0$: ΔG^* is very small compared to ΔG^S, so that

$$\log t \cong \log\frac{\alpha}{I_0} + \frac{\Delta G^S}{k}\frac{1}{T} \tag{11.47}$$

ΔG^S does not depend on *T*. Then we have an asymptote with slope $\Delta G^S / k$.

Let now *y* be the degree of transformation. Then, supposing that α varies between α_{min} and α_{max}, we can write:

$$y = \frac{\alpha - \alpha_{min}}{\alpha_{max} - \alpha_{min}} \tag{11.48}$$

It is interesting to describe the evolution of the transformed phase on a time-temperature diagram. As shown in Figure 11-17, we can draw the curves relative to a given degree of transformation as a function of time and the reciprocal of temperature. For example, the asymptotes obtained α_{min} and α_{max} have a slope $\Delta G^S / k$, following (11.47). In practice, we build and use these diagrams for isothermal transformations.

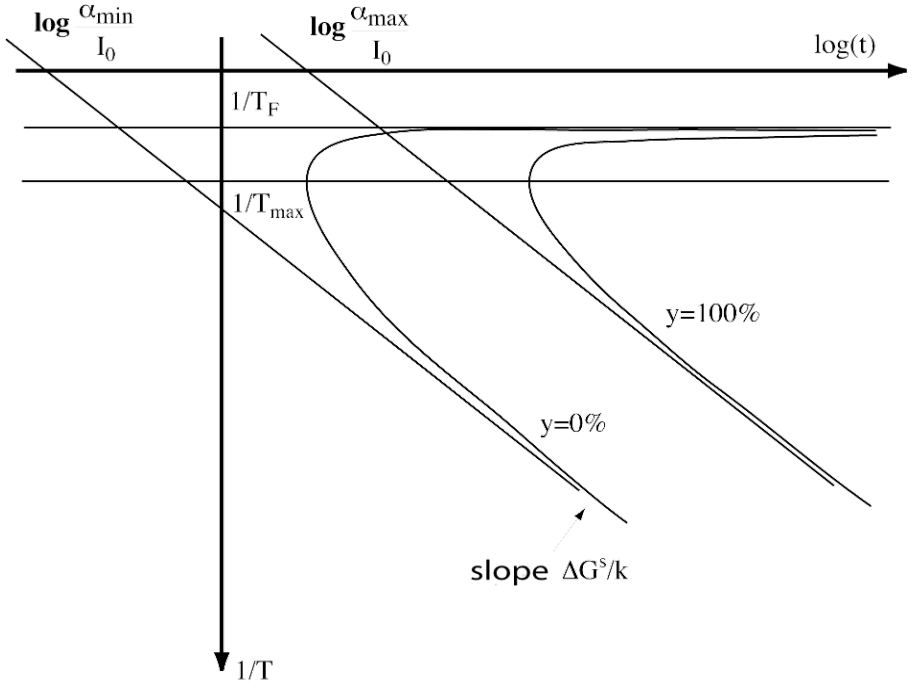

Figure 11-17: *TTT asymptotic diagram*

Rapid quenching

a) Metallic materials

The TTT diagram of nucleation has a nose." Nucleation can be avoided by rapid cooling. However, in the case of pure metals, cooling speeds of 10^6 ˚C/s are insufficient to prevent crystal growth. On the other hand, in alloys, atom redistribution is necessary for nucleation, and amorphous solids (metallic glasses) are formed with very rapid cooling techniques (melt spinning).

b) Non-metallic materials

Inhibiting nucleation of crystalline phases and producing amorphous structures for non-metallic materials (polymers, ceramics) is relatively easy since the structural units of these materials are significant, meaning that forming a grain of critical size is harder (e.g., silicates, glassy oxides, polymers). Thus, the "rapid quenching" of ceramics forms new glassy materials, e.g., $V_2O_5, TeO_2, MoO_3, NO_3$.

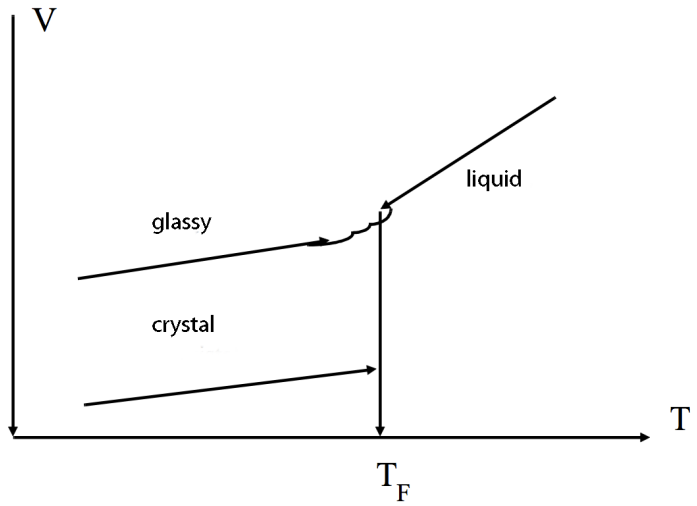

Figure 11-18: *If nucleation occurs during the cooling, we can observe a discontinuity in volume change. Without nucleation, we can observe a discontinuity in the thermal expansion coefficient (change of slope in the curve V=V(T)) associated with forming an amorphous or glassy state.*

11.4.4 Crystal growth

We can mention a specific case of nucleation: the growth of crystals at the interface with a vacuum or a gas. Consider the two extreme cases: a crystalline disordered surface (rough) and an ordered surface (smooth).

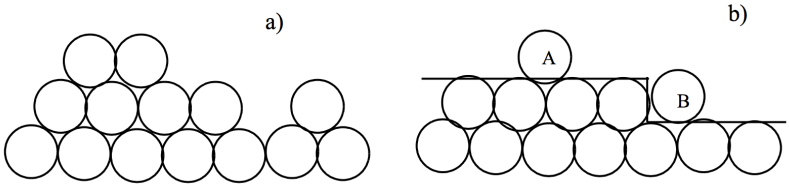

Figure 11-19: *Atomic representation of a) a disordered or rough surface, b) an ordered or smooth surface*

The energy of an atom tends to decrease when the number of surrounding atoms increases. For example, case b) in Figure 11-19 has the minimum energy because the atoms have the maximum number of closest neighbors in that configuration. However, the surface entropy increases with the disorder. Therefore, we have to minimize the surface free energy:

$$G_{surf} = H_{surf} - TS_{surf}$$

- If S_{surf} is predominant, we are in situation a)
- If H_{surf} is predominant, we are in situation b)

The growth of a given interface is achieved through a series of development steps (type B). If all steps are eliminated by growth, new steps are necessary to sustain growth, indicating a significant level of oversaturation. However, experiments show that growth can be observed even with slight oversaturation. This type of growth is explained by the presence of screw dislocations (as discussed in § 6.7 of the textbook).

The nature of the crystal interface depends on the material characteristics and the crystalline nature of the surface. Some crystals grow with ordered surfaces and distinct crystallographic orientations: organic materials, Si, Ge, and ice. On the contrary, metals solidify with surfaces with no particular crystallographic orientation.

11.4.5 Dendritic growth in pure metals

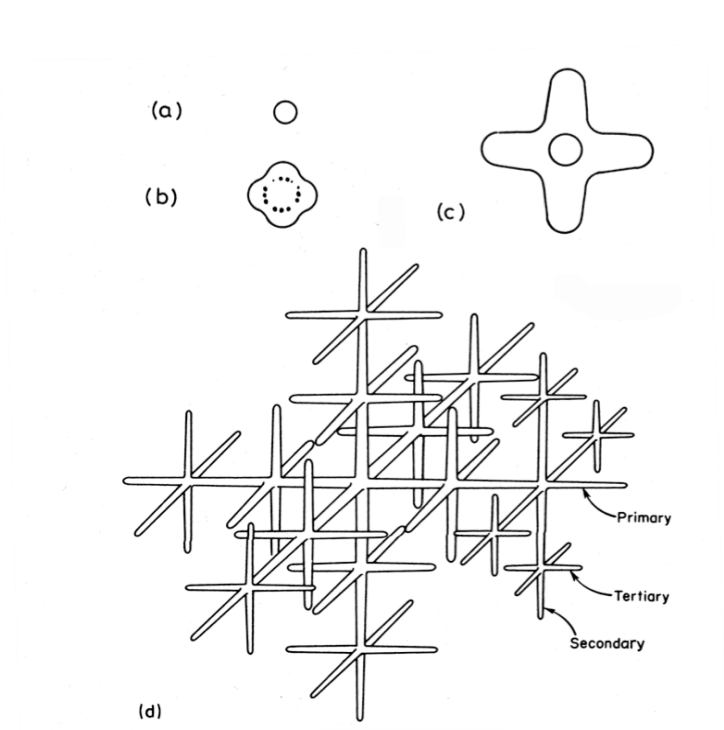

A dendrite corresponds to the particular morphology of a crystal, similar to a tree with its multiple branches. This structure is often observed during solidification.

Dendritic growth occurs only for substances in growth conditions that lead to a disordered solid-liquid interface.

Two cases must be distinguished according to the composition: the growth of dendrites in systems with only one component (pure metals) and the growth in alloys, which is treated in § 11.5.

Figure 11-20: *Dendrite growth scheme. a) Spherical nucleus, b) the interface becomes unstable, c) primary branches, d) secondary branches development.*

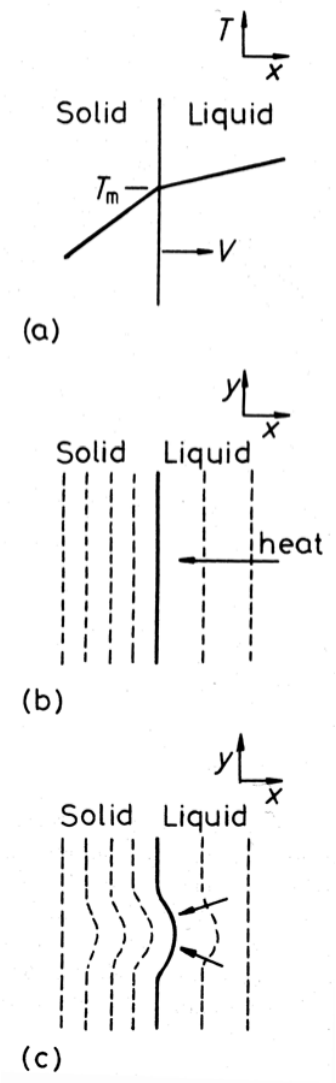

In pure metals, dendritic growth arises from interfacial instabilities driven by supercooling. The degree of supercooling depends only on temperature.

If the liquid is poured into a cold mold, the temperature distribution is similar to that shown in Figure 11-21. The mold walls extract the heat liberated by solidification, and removing this latent heat determines the solidification speed. The heat equation requires that the heat flux J (per unit surface and per unit time) is given by:

$$J = \lambda \overrightarrow{grad}(T) \tag{11.49}$$

Considering the progression of the solid-liquid interface, we can write:

$$\lambda_S \left|\frac{\partial T}{\partial x}\right|_S = L v_i + \lambda_L \left|\frac{\partial T}{\partial x}\right|_L \tag{11.50}$$

where λ_S, λ_L are the thermal conductivities, and v_i is the interface propagation velocity. The heat flux in the solid equals the flux liberated by solidification plus the heat flux from the liquid.

The velocity of propagation of the solidification can be written as:

$$v_i = \frac{1}{L}\left(\lambda_S \left|\frac{\partial T}{\partial x}\right|_S - \lambda_L \left|\frac{\partial T}{\partial x}\right|_L \right) \tag{11.51}$$

Figure 11-21: *Instability of the plane related to the temperature gradient. The temperature gradient (a) stabilizes the planar interface in the present case.*

The heat flux through the solid must be sufficient to extract heat from the liquid and to sustain a positive velocity during solidification. There is always temperature fluctuation or fluctuations in the velocity v_i, which lead to protrusions at the interface. Assume that there is a local variation in the velocity v_i. Since the temperature gradient is inversely proportional to the distance between isotherms, it increases in the liquid and decreases in the solid around the protruded region. This means that the velocity of the interface at the protrusion is lower than that of the plane interface (Figure 11-21). As a result, the protrusion becomes smaller and disappears. The planar interface is then stable.

The situation is different in a supercooled liquid, where the temperature gradients are inverted compared to Figures 11-21. In this case, the heat liberated during the solidification is transferred to the supercooled liquid. As a result, the temperature gradient in the liquid is negative. At the protrusion, isotherms in the liquid are spaced closer than in the solid, and the temperature gradient becomes even more negative. The velocity v_i, determined by (11.51), increases, and the protrusion grows faster than the plane interface.

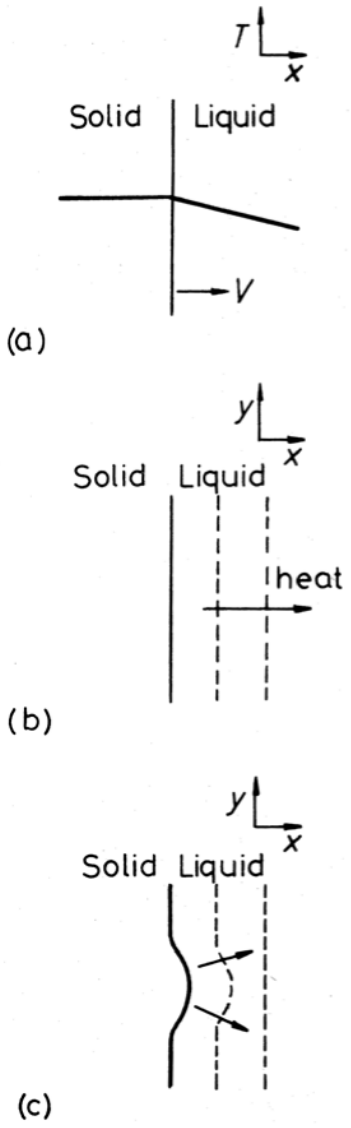

Figure 11-22 : *Instability of the planar front related to the temperature gradient. In the case of supercooling, the temperature gradient (a) destabilizes the planar front and there is a tendency to form a dendrite*

The solid-liquid interface moving into a supercooled liquid is then an instability (a protuberance, as small as it might be) can develop and destroy the planar nature of the interface. As a result, more branches can form, creating a branched tree-like structure called a dendrite.

Remark

The curvature radius of the dendrites must be higher than the critical radius of nucleation (11.38) r_c (stated in another way, the dendrite melts). This phenomenon is illustrated in the paragraph below.

The growth rate of a dendrite

If the latent heat of solidification is rejected only in the liquid, the growth rate is:

$$v_i = -\frac{\lambda_L}{L}\left|\frac{\partial T}{\partial x}\right|_L \qquad (11.52)$$

From the solution to the heat equation in spherical symmetry, we can show that the temperature gradient is given by:

$$\left|\frac{\partial T}{\partial x}\right|_L = \frac{T_\infty - T_i}{\alpha r} = \frac{-\Delta T_c}{\alpha r} \qquad (11.53)$$

with:

T_i = interface temperature
T_∞ = temperature far from the interface
r = curvature radius of the dendrite
α = constant $\cong 1$ if the shape is elliptic

Thus:

$$v_i = \frac{\lambda_L}{L}\frac{\Delta T_c}{\alpha r} \qquad (11.54)$$

This means that as *r* becomes small, v_i increases. Nevertheless, if $r \to 0$ then $v_i \to \infty$, which does not make physical sense, we must consider the nucleation process. For a supercooling of a given ΔT_0, a certain critical radius r_c exists, which guarantees the stability of a nucleus. Any solid region with a radius smaller than r_c is unstable and melts. Therefore, only the domains with $r > r_c$ can grow.

Consider the temperature distribution in front of the dendrite of different curvature radii for a given supercooling of ΔT_0 (Figure 11-23).

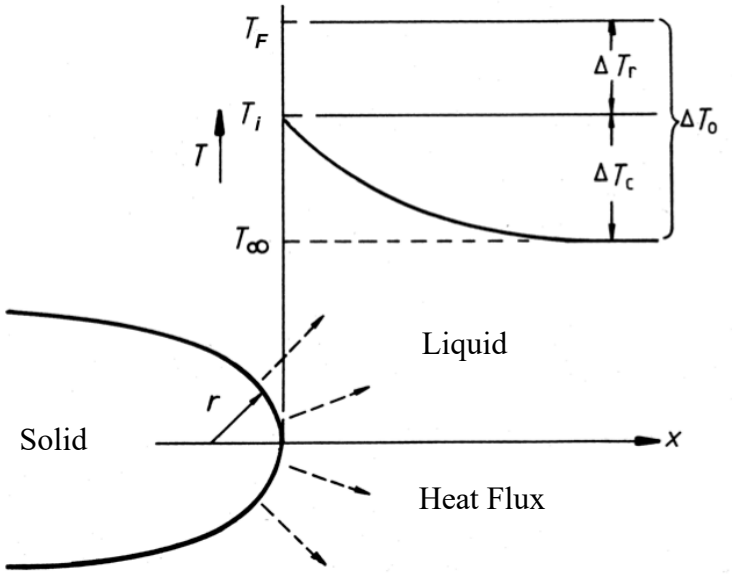

Figure 11-23: *Growth of a dendrite by supercooling*

The equilibrium temperature of the interface T_i depends on the curvature radius *r*.

$$r = \frac{2\gamma_{SL}}{L}\frac{T_F}{T_F - T_i} = \frac{2\gamma_{SL}}{L}\frac{T_F}{\Delta T_r} \tag{11.55}$$

We define them according to (11.38):

r is minimum if $T_i = T_\infty$ and then $\Delta T_r = \Delta T_0$ and $r = r_c$.
r tends to infinity if $T_i \to T_F$ and thus $\Delta T_r \to 0$. This means that if the interface does not remove enough heat, the driving force for dendritic growth stops.

We can then write that:

$$\Delta T_r = \Delta T_0 \frac{r_c}{r} \tag{11.56}$$

As $\Delta T_0 = \Delta T_r + \Delta T_c$, we can write:

$$\Delta T_c = \Delta T_0 \left(1 - \frac{r_c}{r}\right) \tag{11.57}$$

For $r = r_c$, (r_c being the critical radius corresponding to the supercooling ΔT_0), $\Delta T_c = 0$.

if $r > r_c$ $T_i > T_\infty$ as solidification releases heat
if $r < r_c$, $T_i < T_\infty$ because fusion absorbs heat. In this case, the dendrite melts.

The growth rate of the dendrite is, according to (11.54):

$$v_i = \frac{\lambda_L \Delta T_0}{L\alpha r}\left(1 - \frac{r_c}{r}\right) \tag{11.58}$$

We note that the propagation velocity at the dendrite's tip tends to zero for $r \to r_c$ and for $r \to \infty$ where the conduction becomes too slow. The maximum velocity v_{max} is obtained for dendrites with a radius close to $2r_c$. We can deduce a distance between branches of roughly $4r_c$.

11.5 Solidification of binary alloys

In § 11.4, we have discussed the case where the driving force of the solid phase growth was the degree of supercooling of the liquid phase ΔT_0. However, when we consider alloys, the situation is quite different: the concentration gradients and, thus, diffusion become the main driving forces of solidification. In particular, diffusion in the liquid phase, which is 3 or 4 orders of magnitude faster than in the solid phase, determines the structure of solidification observed in materials. We can distinguish 3 cases:

1) Slow solidification at thermodynamic equilibrium,
2) Solidification at the thermodynamic equilibrium of the liquid phase and negligible diffusion in the solid phase,
3) Solidification is regulated by diffusion in the liquid phase.

We consider a eutectic phase diagram in which the boundaries between the liquid and solid phases are straight lines (equation 11-24), allowing a more straightforward analysis. Thus, we can write:

$T = k_S X_S + T_0$ for the limit of the solid phase (solidus) (11.59)

$T = K_L X_L + T_0$ for the limit of the liquid phase (liquidus) (11.60)

For a temperature T (horizontal section of the phase diagram in Figure 11-24):

$$X_S = \frac{k_L}{k_S} X_L = kX_L \quad \text{with (k<l).} \tag{11.61}$$

We also have $X_L = \frac{k_S}{k_L} X_S = \frac{X_S}{k}$.

We note in particular that for a concentration X_0, the limit of the liquidus is located at $\frac{X_0}{k}$. The limit of the solidus at kX_0.

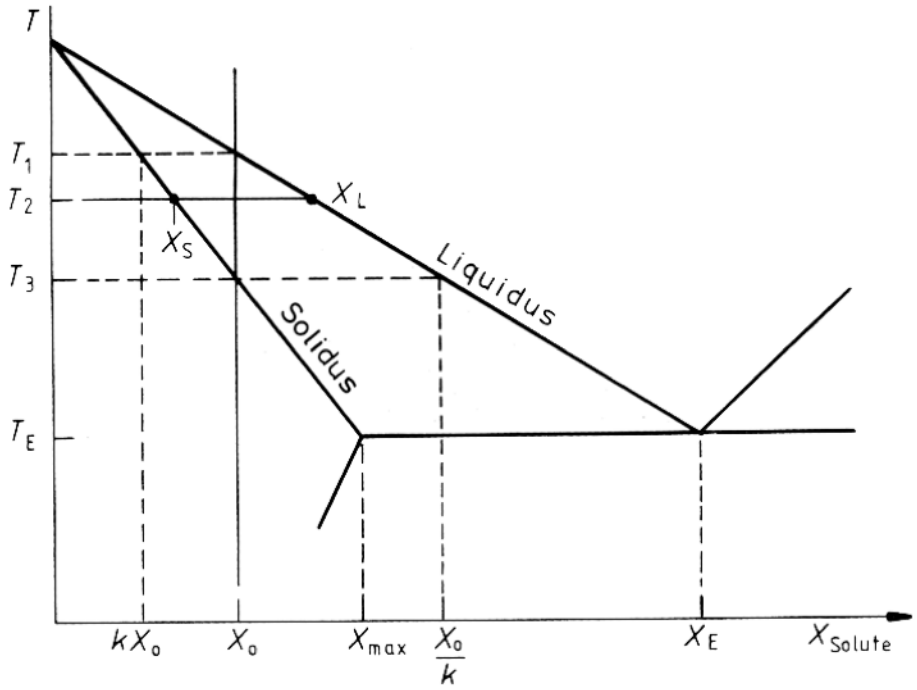

Figure 11-24: *Model phase diagram (Xs=kXL)*

In this case, we examine the distribution of solute (atoms B) in the liquid and solid phases (α+β) as a function of concentration X in A. We can imagine an ideal experiment in which we measure the composition of a bar as the solidification front proceeds at velocity *v*.

11.5.1 Thermodynamic equilibrium

It is the case in which the cooling rate is sufficiently low to allow the solid phase to reach its equilibrium state by diffusion. The composition of the solid and the liquid is determined at all times by the equilibrium diagram. At the temperature T_3, all the solids have the initial concentration X_0.

11.5.2 Thermodynamic equilibrium in the liquid - no diffusion in the solid

It is the (realistic) case in which diffusion in the liquid is sufficiently high compared to the cooling rate, so a perfect mixture of the constituents is maintained. As the temperature decreases, the liquid becomes richer in solute, whereas the solid is impoverished compared to the equilibrium line (Figure 11-25).

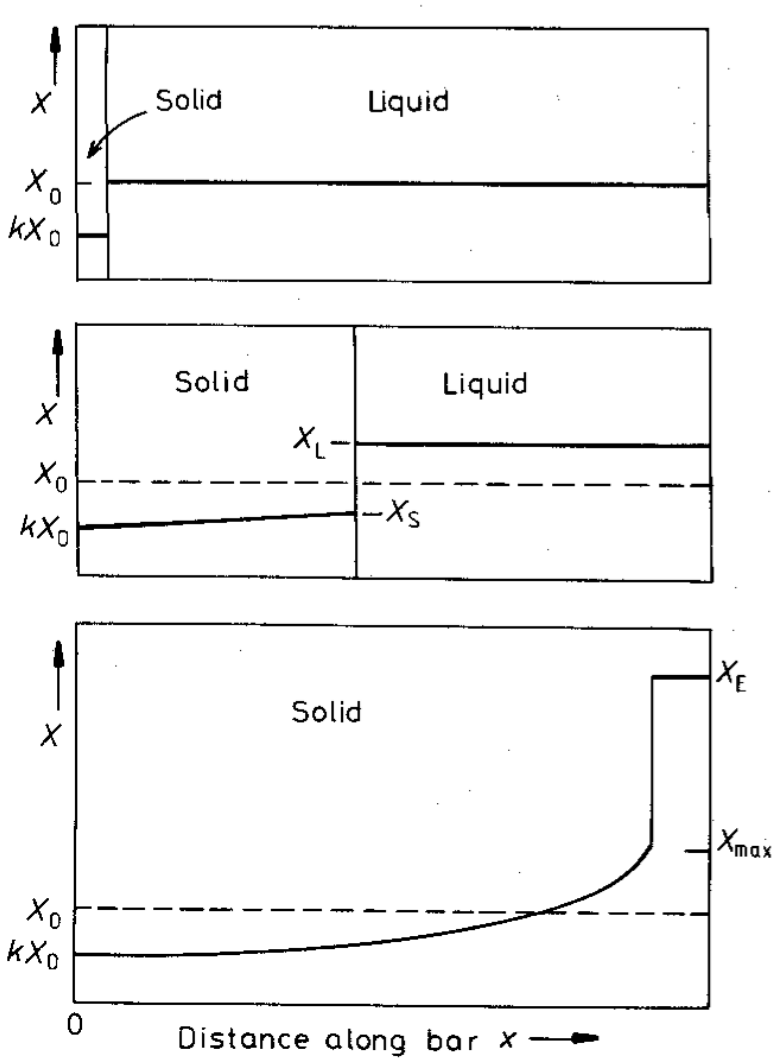

Figure 11-25: *Schematic composition of phases during the solidification of a bar (monocrystal)*

We can show (exercise) that the concentration in the solid follows the law (Scheil equation):

$$X_S = kX_0(1-f_S)^{(k-1)} \tag{11.62}$$

And the concentration in the liquid:

$$X_L = X_0(f_L)^{(k-1)} \tag{11.63}$$

where f_L and f_S are, respectively, the fractions of the liquid and solid phases.

We note that, for $k<1$, these functions predict a sharp increase in the concentration upon complete solidification: the last drops of liquid solidify with an eutectic composition (Figure 11-25).

11.5.3 solidification controlled by diffusion in the liquid phase

We consider the case where the solute concentration in the solid phases controls diffusion in the liquid. At steady-state, the quantity of solute rejected in the liquid during solidification must be evacuated by a flux corresponding to the concentration gradient in the liquid. We can write:

$$vX_S = vX_L + D_L \frac{\partial X_L}{\partial x} \tag{11.64}$$

where v is the velocity of the solidification front (assumed planar) and D_L is the diffusion coefficient in the liquid. Taking into account the assumption that $X_S = kX_L$, the solution of equation (11.64) for a steady-state velocity yields:

$$X_L(x) = X_0\left[1+\frac{1-k}{k}\exp\left(-\frac{(1-k)}{(D_L/v)}\right)\right] \tag{11.65}$$

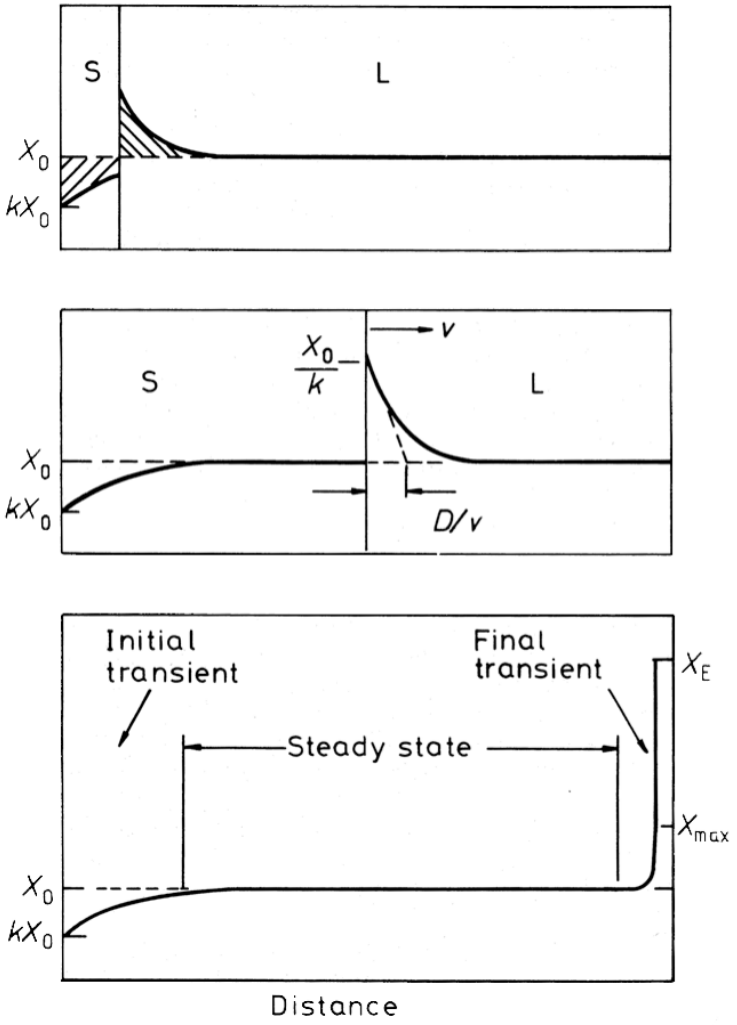

Figure 11-26: *Schematic composition of phases during the progressive solidification of a bar (monocrystal). The velocity v is chosen so that a steady state is reached.*

The concentration of the liquid is $\frac{X_0}{k}$ at the solidification front and decreases exponentially to X_0 far from the interface.

The liquidus is the equilibrium temperature at which a liquid and a solid coexist. If k_L is the slope of the liquidus, the temperature of the liquid at the concentration X_L equals (11.60):

$$T_e = T_0 + k_L X_L \tag{11.66}$$

The temperature profile at equilibrium before the interface (located at x=0) is then:

$$T_e = T_0 + k_L X_0 \left[1 + \frac{1-k}{k} \exp\left(-\frac{(1-k)}{(D_L / v)} \right) \right] \tag{11.67}$$

The actual temperature in the liquid, T_r, is:

$$T_r = T_i + \left| \frac{\partial T}{\partial x} \right|_L x = T_0 + k_L \frac{X_0}{k} + \left| \frac{\partial T}{\partial x} \right|_L x \tag{11.68}$$

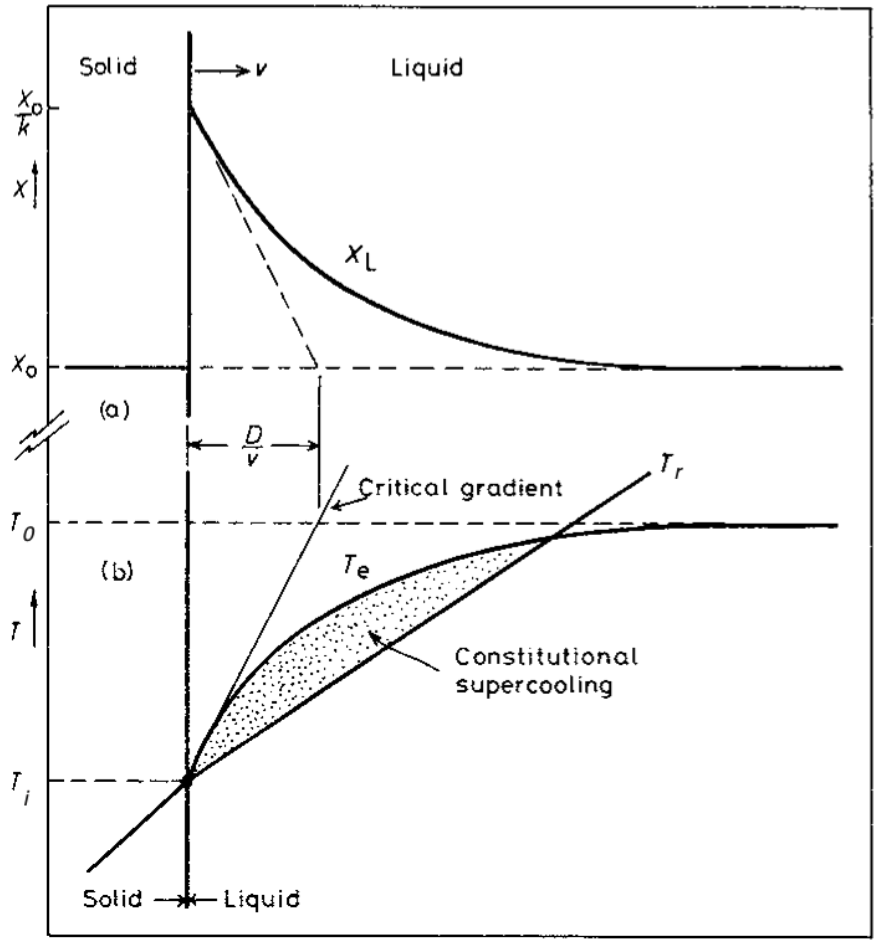

Figure 11-27: *The comparison between T and T shows that part of the liquid has to be in supercooling*

The liquid is then out of equilibrium compared to its concentration. This supercooling results from the concentration gradient in the liquid and is called **constitutional supercooling**.

This supercooling zone does not exist if the slope of the line giving the actual temperatures is higher than the slope of the tangent to the curve T_e. That is to say, if

$$\left|\frac{\partial T}{\partial x}\right|_L > \frac{k_L X_0}{D_L}\frac{(1-k)^2}{k} \tag{11.69}$$

The difference between the actual and equilibrium temperatures is illustrated in Figures 11-27.

11.6 Solidification structures of alloys

In the case of pure metals, two kinds of solid-phase growth exist: normal to the surface plane and the dendritic growth direction. However, in alloys, in addition to these two solidification processes, we also have cellular growth, which depends solely on constitutional supercooling.

11.6.1 Cellular texture

The solid-liquid interface presents a lattice of hexagonal cells (Figure 11-28). This structure can be explained by solidification, which produces an excess of solute in the liquid.

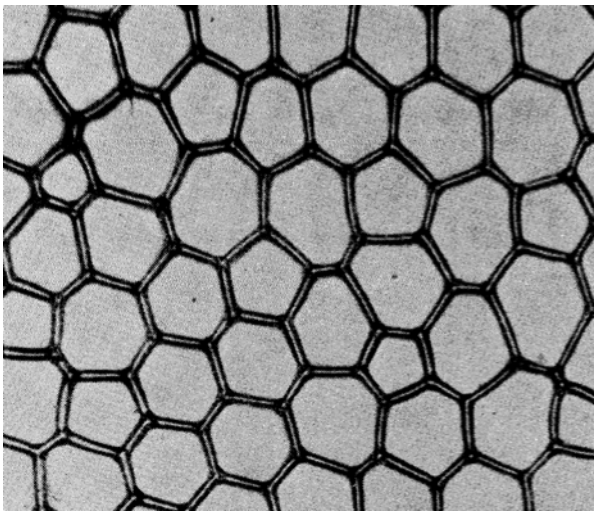

Figure 11-28: *Cellular texture of an Sn-Pb alloy*

When a protuberance develops in the liquid, the convex surface produces lateral and longitudinal concentration gradients. The excess solute accumulates around the base of the protuberance, lowering the solidification temperature in this region (Figure 11-29). The protuberance does not spread laterally. The solute concentration in the liquid can reach the eutectic composition, leading to the solidification of cells of the α phase surrounded by a eutectic composite of α+β.

Remark

In such conditions, without supercooling, a solidified alloy forms a pure metal, i.e., a planar front growing normal to the liquid-solid interface.

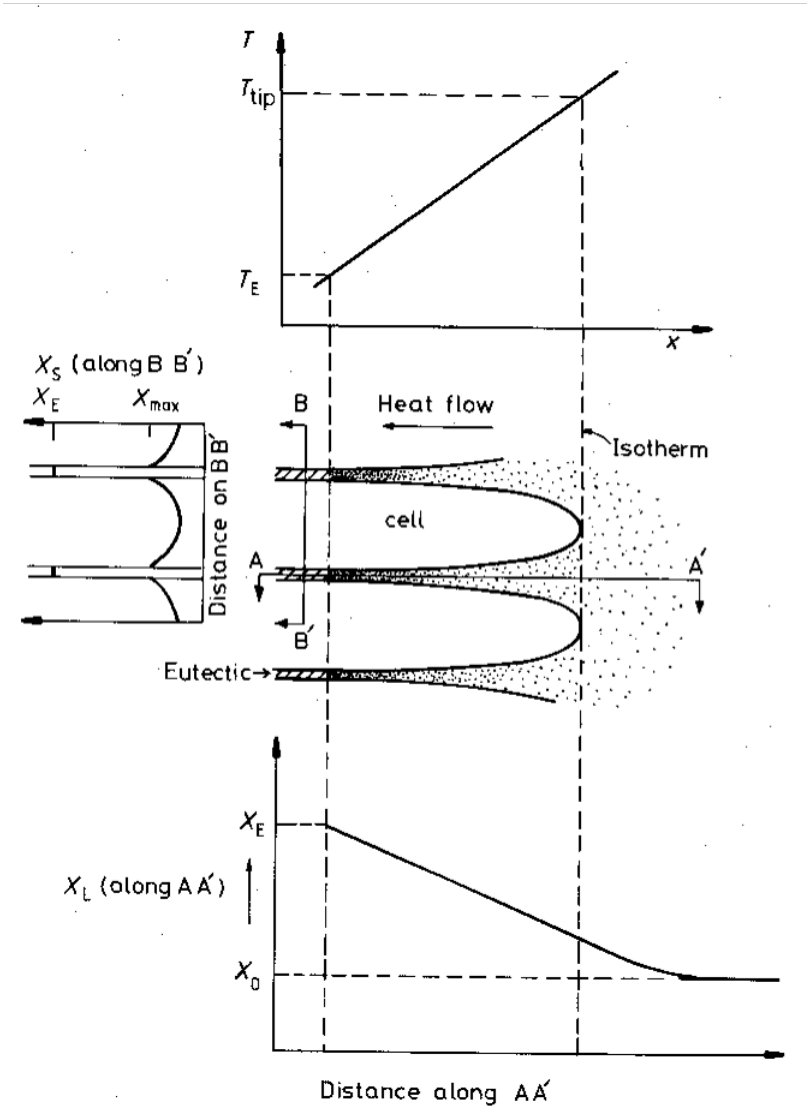

Figure 11-29: *The growth of a cellular structure is related to the constitutive supercooling*

11.6.2 Dendritic texture

The cellular texture appears at the limit of the constitutive supercooling. Increasing the supercooling (constitutive or thermal cooling) produces a dendritic texture (Figure 11-30b). Indeed, growth is controlled by the velocity at which the solute is removed from the interface. The velocity of the interface is proportional to the concentration gradient (11.64).

$$v_i = -D_L \frac{\partial X_L}{\partial x} \frac{1}{(X_L - X_S)}$$

The concentration gradient of the solute is more substantial and closer to the protuberance. Thus v_i it is more significant at this location, and the interface is unstable. This results in the passage to dendritic growth.

We observe the formation of primary, secondary, and tertiary dendrites, and so on. Dendrites are an example of a fractal structure. The formation of dendrites is also related to the preferential orientations of crystals.

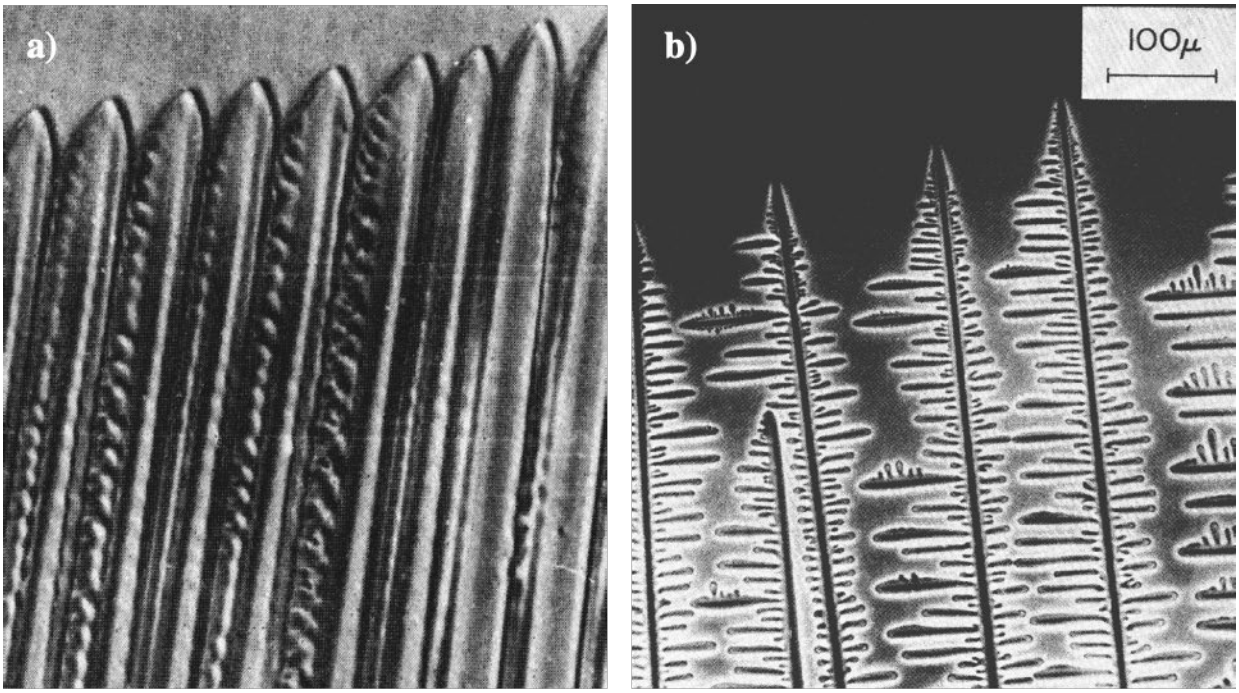

Figure 11-30: *Growth of cells in CBr_4 (a) and passage to a dendritic structure (b)*

11.6.3 Eutectic solidification

The eutectic reaction is of the kind: $L \rightarrow \alpha + \beta$. Eutectic alloys can show different morphologies, as in Figure 11-31: lamellar (a), rod-like (b), globular (c), or acicular (d).

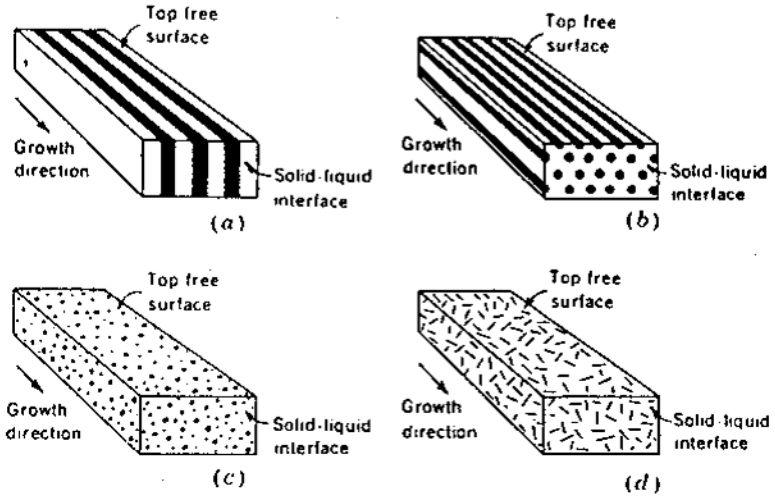

Figure 11-31: *Morphology of eutectic structures*

From an energy perspective, the most stable configuration is the globular shape, as it has the lowest surface-to-volume ratio. However, this texture requires repeated nucleation of the second phase. Therefore, the lamellar structure is the most common one since, in this case, the two phases grow cooperatively, and the need for a nucleation process is reduced.

Growth of lamellar eutectics

The free energy (per unit volume) during the reaction $L \rightarrow \alpha + \beta$ is expressed as a function of the parameter λ (distance between the phases α and β, in the form of lamellae).

$$g(\lambda) = g(\infty) + \frac{\gamma_{\alpha\beta} S_{\alpha\beta}}{V} = g(\infty) + \frac{2\gamma_{\alpha\beta}}{\lambda} \tag{11.70}$$

This formula accounts for the interface formation energy between the lamellae.

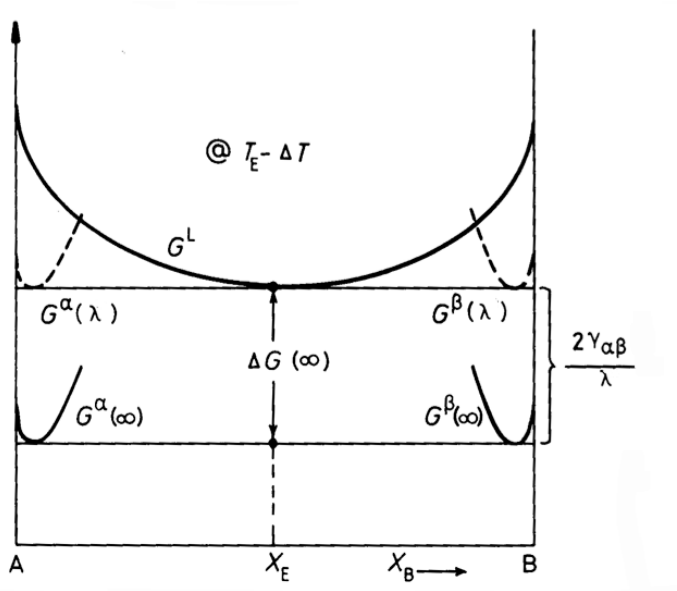

Figure 11-32: *Energy diagram during the formation of a eutectic with spacing λ between the lamellae*

We have an increase in the free energy of the solid when λ, the distance between the lamellae, decreases. This shifts the eutectic melting point to lower temperatures. For a given ΔT, a critical distance λ_c exists such that L, α, and β are in equilibrium at $T_E - \Delta T$. Consider the concentration gradients in front of the lamellae α and β. At the interface L-α, the liquid is rich in B atoms, whereas at the interface L-β, the liquid is rich in A atoms. Atoms B diffuse then from the lamellae α towards the lamellae β, and the A atoms in the opposite direction.

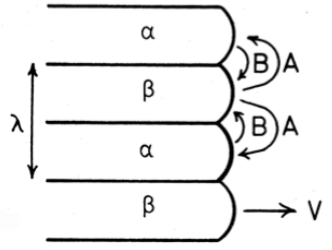

Figure 11-33: *Growth of eutectic lamellae with diffusion in the liquid*

The average concentration gradient in the liquid between the lamellae α and β is:

$$\frac{\Delta X}{\lambda/2} = \frac{2(X_B^{L-\beta} - X_B^{L-\alpha})}{\lambda} \tag{11.71}$$

If the interface moves by *dx* during a time *dt*, a quantity of atoms B equal to $(X_B^{L-\alpha} - X_B^{\alpha})dx$ is rejected in the liquid at the interface with the α phase. Proceeding in the same way leads to equation (11.64):

$$(X_B^{L-\alpha} - X_B^{\alpha})v = \frac{-2D_L(X_B^{L-\beta} - X_B^{L-\alpha})}{\lambda}$$

and thus:

$$v_\alpha = v_\beta = \frac{2D_L(X_B^{L-\alpha} - X_B^{L-\beta})}{\lambda(X_B^{L-\alpha} - X_B^{\alpha})} \tag{11.72}$$

Therefore, v_α grows if λ decreases. But when $\lambda = \lambda_c$, that is to say, $X_B^{L-\alpha} = X_B^{L-\beta}$, v_α tends to zero.

We can then write: $\Delta X = \Delta X_0\left(1 - \frac{\lambda_c}{\lambda}\right)$ and thus:

$$v_\alpha = v_\beta = \frac{2D_L\Delta X_0}{\lambda(X_B^{L-\alpha} - X_B^{\alpha})}\left(1 - \frac{\lambda_c}{\lambda}\right) \tag{11.74}$$

The maximum velocity is for $\lambda = 2\lambda_c$.

We can verify that $\lambda_c \cdot v_{max} = const$

In practice, we use the relation (11.74) to adjust the spacing between the lamellae: as v increases, λ must decrease (Figure 11-34).

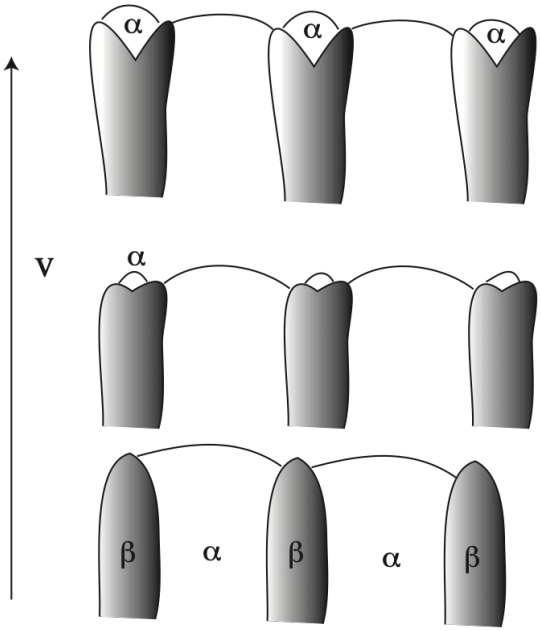

Figure 11-34: *Growth of secondary lamellae when the forward velocity of the solidification front increases, the gap between the lamellae decreases*

Example of a eutectic structure: pearlite

A typical example of a eutectic structure is pearlite in carbon steel. This is a transformation occurring in the solid state. Since diffusion essentially governs it, the formalism developed previously remains valid. We can observe the progression in the austenite of ferrite and cementite (Fe_3C) lamellae (Figure 11-35).

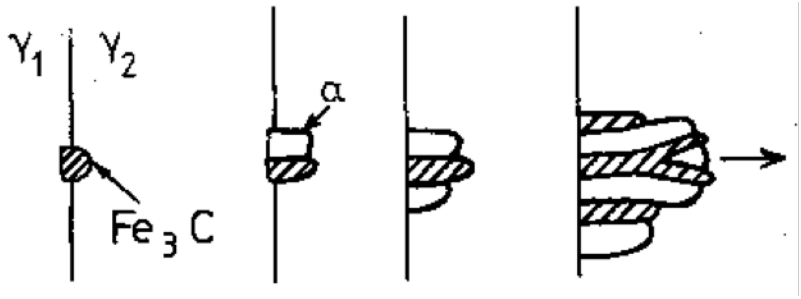

Figure 11-35: Growth diagram of perlite

The transformation begins at the austenite grain boundaries. We can initially have either a cementite nucleus or a ferrite nucleus. If the ferrite transforms first, carbon is absorbed from the austenitic phase into the ferrite. This reduces the stability of the austenitic phase, leading to ferrite formation. Growth occurs cooperatively via carbon transfer from ferrite to cementite. Hemispherical colonies are formed and propagated until they reach a neighboring colony (Figure 11-36).

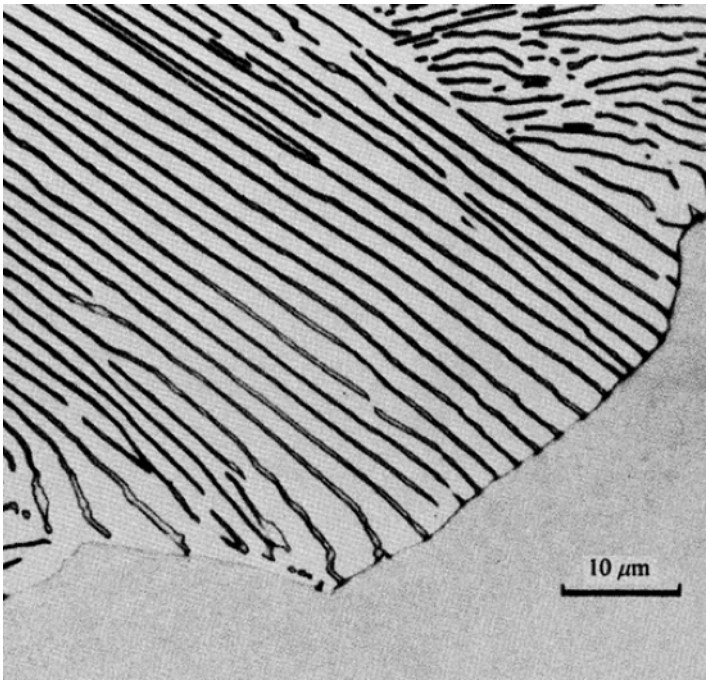

Figure 11-36: *Perlite growth in austenite*

11.7 Solidification of a bar

Many alloys are cast as bars in a mold. The solidified matter is then used as a base for machining processes. Knowing the crystal structure of the bar, which can be quite non-homogeneous, is crucial. Most metals shrink when they solidify. This cannot be avoided, but must be controlled in foundry operations.

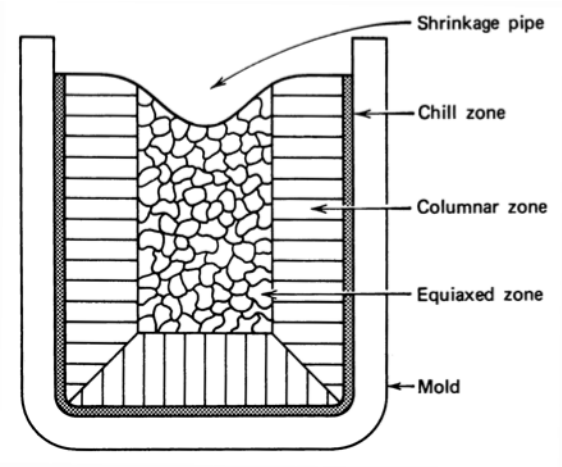

Figure 11-37: *Solidified bar in a mold. We can observe a withdrawal in the last solidified zone.*

If heat is extracted only from the bottom of the mold, the solidification interface remains flat, and there are no shrinkage cavities. On the other hand, if the face is exposed to the air and has a poor heat transfer rate, a pipe cavity will form.

Suppose the free surface does expel heat well. In that case, we can observe the formation of a crust on the free surface, and the delayed solidification beneath the surface results in the formation of porosities due to shrinkage. These porosities appear between the dendrites. They do not generally cause problems because they are eliminated by rolling.

11.7.1 Crystallisation of the bar

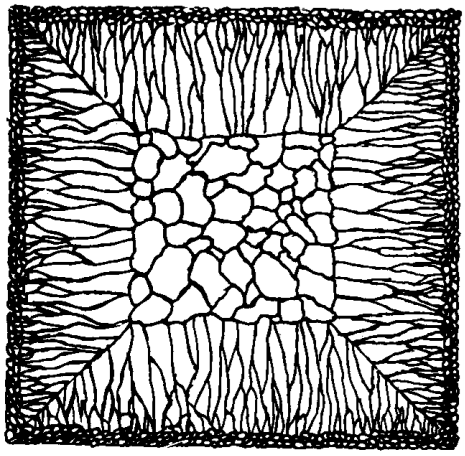

Figure 11-38: *Solidification structure schematic based on experimental images*

In general, we can set apart three different zones in the solidified bars:

i) A layer of metal solidifies first on the walls of the mold. Here, the supercooling is high, so nucleation is easier. As a result, we have many nuclei, forming many small, non-oriented crystals.

ii) As the solidification layer thickens, the temperature gradient decreases, and thus the nucleation rate decreases. These conditions (limited supercooling but still high-temperature gradients) are ideal for developing large oriented crystals (basaltic texture).

iii) Heat expulsion slows toward the end of solidification, and the temperature is relatively homogeneous. We can then observe the formation of large crystals without preferential orientation at the bar's core.

Segregation

During the solidification of an alloy, the liquid gets richer in solute. The portion of the liquid that solidifies last is the one most enriched in solute. As a result, we can observe a greater concentration at the heart of the bar (*macrosegregation*). Furthermore, we showed (in § 11.6) another form of segregation observed at the dendrite level (*microsegregation*).